Application of quasi-degenerate perturbation theory to the calculation of rotational energy levels of methane vibrational polyads

Patrick Cassam-Chenaï, Guillaume Rousseau, Amine Ilmane, Yann Bouret, Michaël Rey

Application of quasi-degenerate perturbation theory to the calculation of rotational energy levels of methane vibrational polyads

P. Cassam-Chenaï,[1, a)] G. Rousseau,[1] A. Ilmane,[1] Y. Bouret,[2] and M. Rey[3]

[1)] *Univ. Nice Sophia Antipolis, CNRS, LJAD, UMR 7351, 06100 Nice, France.*

[2)] *Univ. Nice Sophia Antipolis, CNRS, LPMC, UMR 7336, 06100 Nice, France.*

[3)] *Groupe de Spectrométrie Moléculaire et Atmosphérique, CNRS UMR 6089, BP 1039, F-51687 Reims Cedex 2, France.*

(Dated: 16 April 2015)

In previous works, we have introduced an alternative perturbation scheme to find approximate solutions of the spectral problem for the rotation-vibration molecular Hamiltonian. The convergence of our method for the methane vibrational ground state was very satisfactory and our predictions were quantitative. In the present article, we provide further details on the implementation of the method in the degenerate and quasi-degenerate cases. The quasi degenerate version of the method is tested on excited polyads of methane, the results are assessed with respect to a variational treatment. The optimal choice of the size of quasi-degenerate spaces is determined by a trade-off between speed of convergence of the perturbation series and the computational effort to obtain the effective super-Hamiltonian.

[a)]Electronic mail: cassam@unice.fr

I. INTRODUCTION

Recorded spectra arising from molecular species is a major source of information on many objects of astrophysical or atmospheric interest. The detections and observations of a quickly increasing number of such objects with hot atmospheres, (for example Brown Dwarfs or "Hot Jupiter" type of extrasolar planets), challenge our understanding of the spectra of many molecules and emphasize the limits of existing spectroscopic databases. Computational spectroscopy by using *ab initio* quantum chemical methods or combinations of such methods with empirical datas, has addressed this challenge and made valuable contributions to the analysis and predictions of molecular rotation-vibration spectra in recent years[1].

Variational *ab initio* calculations are often considered as the supreme way of achieving high accuracy and reliability of the predicted spectra. However, when billions of eigenvalues are required to model all populated quantum energy levels at high temperature, such an approach ceases to be applicable. However, one can switch to pertubational approaches. It is noteworthy to mention that the Ritz variational approach often used in the context of rotation-vibration calculation, can be regarded as a particular case of first order quasi-degenerate perturbation theory[2]. So the latter encompasses the former.

The purpose of this article is to further develop our generalized Rayleigh-Schrödinger pertubation method, which has proved very accurate for methane vibrational ground state, to the case of quasi-degenerate states, in order to tackle the crowded, high energy regions of molecular rotation-vibration spectra. The extension of the method leads to effective super-Hamiltonian simultaneously modelling the rotational sublevels of a set of vibrational levels considered has quasi-degenerate.

Gathering vibrational energy levels into a quasi-degenerate set is somewhat arbitrary. So, a large part of the article is devoted to the study of the optimal choice of such a set, in terms of accuracy versus compuational effort, from minimal sets corresponding to sets of exactly degenerate levels, to the largest possible set that is the set of all calculated vibrational levels. The latter case corresponds at first order of perturbation as already mentionned to the Ritz variational method also known as the configuration interaction method in quantum chemistry.

To perform such study, we have chosen methane, as for our ground state studies[2–4]. This molecule is an important greenhouse gaz in the Earth's atmosphere and it is of particular interest for the study of solar system giant planets and some of their satellites such as Titan, some exoplanets and some Brown Dwarfs[5–13]. The high symmetry of

methane main isotopologue has for consequences the occurence of exactly degenerate levels in its spectrum and this can be exploited for debugging purposes. Also, the "polyad" structure of the spectrum, associated to the approximate quantum number, $P = n_2 + n_4 + 2n_1 + 2n_3$, (where n_i is the number of quanta in vibrational mode i in conventional spectroscopic ordering) is an interesting feature to test our quasi-degenerate perturbation method, as we shall see. Over the past 30 years, line-by-line analyses have been performed using a symmetry-adpated formalism developed and implemented in Dijon, Tomks and Reims groups[14–16]. About 21400 line transitions of $^{12}CH_4$ have been assigned and 10100 measured line intensities were included in empirical models[17]. Up to $P = 3$, the analysis of room-T spectra is almost complete while for $P = 4$, only about 25% of vibrational sublevels have been explored[18]. Recently, a large experimental effort has been devoted to extend measurements of methane spectra for $P = 5$ using laser techniques[19].

Various issues concerning theoretical methane spectra predictions from PES and DMS have already been discussed[20–29]. We have decided to focus our study on the "tetradecad" that is the polyad associated to $P = 4$, since it is the lowest one for which spectroscopic analysis is still considered as insufficiently accurate. Within the tetradecad, we will use the intense $2\nu_3$ vibrational band which has been thoroughly studied experimentally and has been chosen to monitor methane from space by the MERLIN lidar mission[30], to assess convergence.

The article is organized as follows: In the next section, the theory is exposed and the formulas implemented in our computer code are derived. Then, the theory is applied to the $2\nu_3$ band of methane main isotopologue, for quasi-degenerate vibrational spaces of increasing sizes and perturbation orders up to 4 in the case of the smallest quasi-degenerate spaces. Results are compared to configuration interaction reference values. We conclude that variational accuracy can be achieved at reduced computational cost by adjusting pertubation order and the size of the quasi-degenerate space.

I. *AB INITIO* EFFECTIVE ROTATIONAL SUPER HAMILTONIAN AND DIPOLE MOMENT SUPER OPERATOR

In this section, the theory of effective operators implemented in this work is briefly introduced, in order to make the article self-contained. Effective Hamiltonian theory has a long history, and many reviews of this topics are available, see[31–33] to quote a few. Our generalized Schrödinger equation need not be solved pertubationally, however the pertu-

bative solutions of the present section can be seen as a particular case of Ref.[33] section 8. The specific properties of this particular perturbation theory are detailed in[31], where its origin is traced back to Des Cloizeaux in 1960[34]. An independent formulation using the wave operator idea can be found in[35]. This theory has also been shown equivalent[31] to the contact transformation approach of Van Vleck[36], Kemble[37] and Primas[38], provided a minimum distance criterium between the eigenkets of the original and tranformed representations is enforced, and to the approach of Buleavski[39]. However, there is one more ingredient in our approach: the fact that the tensorial structure of the Hilbert space of quantum states is compatible with the decomposition of the Hamiltonian into a "main" and a "perturbative" contribution. Note that this ingredient has also been exploited in[32] in the framework of the contact transformation formalism.

A. Definition of effective operators

Let us consider a Hamiltonian, $H(X,Y)$, acting on a Hilbert space having a tensorial structure, $V = V_{\mathbf{x}} \otimes V_{\mathbf{y}}$, and built with two sets of operators: set X containing operators acting on $V_{\mathbf{x}}$ and set Y containing operators acting on $V_{\mathbf{y}}$. In Dirac notation, kets on V (resp. on $V_{\mathbf{x}}$, $V_{\mathbf{y}}$) will be denoted by $|\cdots\rangle$, (resp. $|\cdots\rangle_{\mathbf{x}}$, $|\cdots\rangle_{\mathbf{y}}$). No index will be used for the corresponding bra's. The identity on $V_{\mathbf{x}}$ (respectively $V_{\mathbf{y}}$) will be written $Id_{\mathbf{x}}$ (respectively $Id_{\mathbf{y}}$). The action of an operator $O_{\mathbf{x}} \in X$ (respectively $O_{\mathbf{y}} \in Y$) is extended to V by tensorial multiplication with the identity $Id_{\mathbf{y}}$ (respectively $Id_{\mathbf{x}}$): $O_{\mathbf{x}} \to O_{\mathbf{x}} \otimes Id_{\mathbf{y}}$ (respectively $O_{\mathbf{y}} \to Id_{\mathbf{x}} \otimes O_{\mathbf{y}}$).

Our motivation for developing this theory stems from the molecular rotation-vibration Hamiltonian in the Eckart frame. Let denote by X the set of vibrational coordinates and their conjugate momenta, $X = \{(Q_i)_i, (P_k)_k\}$, and by Y, the set of Euler angles and their conjugate momenta, $Y = \{\theta, \chi, \phi, P_\theta, P_\chi, P_\phi)\}$. The operators in X act on the Hilbert space, $V_{\mathbf{x}}$, of square integrable functions (over the appropriate integration domains) of the vibrational degrees of freedoms (DOF), collectively denoted by $\mathbf{x}$. Similarly, those in Y act on the Hilbert space, $V_{\mathbf{y}}$, of square integrable functions of the rotational DOF, $\mathbf{y}$. The Hilbert space of the whole system is the tensor product, $V = V_{\mathbf{x}} \otimes V_{\mathbf{y}}$.

The Hamiltonian of the system, $H(X,Y)$, considered in this work will be the Eckart-Watson Hamiltonian for non linear molecules[40]. It can be decomposed as,

$$H(X,Y) = H_0(X) \otimes Id_{\mathbf{y}} + H_1(X,Y), \tag{1}$$

where, in atomic units, $H_0(X)$ is the $(J=0)$-Hamiltonian,

$$H_0(X) = \frac{1}{2}\sum_k P_k^2 + U + \frac{1}{2}\sum_{\alpha\beta}\mu_{\alpha\beta}\pi_\alpha\pi_\beta - \frac{1}{8}\sum_\alpha \mu_{\alpha\alpha}, \tag{2}$$

and,

$$H_1(X,Y) = \sum_{\alpha\beta}\frac{1}{2}\mu_{\alpha\beta}\otimes\Pi_\alpha\Pi_\beta - \mu_{\alpha\beta}\pi_\alpha\otimes\Pi_\beta. \tag{3}$$

In the equations above, U is the potential of electronic origin in the Born-Oppenheimer approximation, expressed as a function of the normal coordinates Q_i, μ is the 3 by 3 effective reciprocal inertia matrix whose series expansion in terms of the normal coordinates is

$$\mu = \sum_{r=0}^{+\infty}\left(\frac{1}{2}\right)^r (r+1)\sum_{k_1,\ldots,k_r} I_e^{-1}a_{k_1}I_e^{-1}\ldots a_{k_r}I_e^{-1}Q_{k_1}\ldots Q_{k_r}, \tag{4}$$

where, I_e^{-1} is the inverse of the inertia tensor $I(Q_1,...,Q_n)$ at equilibrium and $(a_k)_k$ the derivatives of the latter with respect to the normal coordinates,

$$a_k = \left(\frac{\partial I}{\partial Q_k}\right)_0. \tag{5}$$

π is the so-called "Coriolis coupling operator", it only depends upon the operators in set X. Π is the total angular momentum, and is the sole quantity depending upon the operators in set Y.

Let $(\psi_n)_n$, be a normalized Hilbertian basis set of $V_{\mathbf{x}}$, we have: $Id_{\mathbf{x}} = \sum_n |\psi_n\rangle_{\mathbf{x}}\cdot\langle\psi_n|$. In view of the applications, we use for each basis function ψ_n, a possibly different $\mathbf{y}$-basis set, $(\Psi_K^n)_{n,K}$ to construct a tensor basis set for V, $(\psi_n\otimes\Psi_K^n)_{n,K}$. For all n, we will have, $Id_{\mathbf{y}} = \sum_K |\Psi_K^n\rangle_{\mathbf{y}}\cdot\langle\Psi_K^n|$.

Since we are free to choose the basis set of $V_{\mathbf{x}}$, we can take for $(\psi_n)_n$ a set of orthonormal eigenvectors of $H_0(X)$. We label this set with positive integers such that the associated eigenvalues $(\nu_n)_n$ be in increasing order.

The novelty in the present article with respect to previous publications, is that we consider the case where one has to treat several vibrational bands, usually degenerate or quasi-degenerate, together to obtain physically meaningful results. For example, in methane, it is well known that the vibrational bands form so-called "polyads"[41]. In each polyad, the ro-vibrational states are strongly coupled and cannot be dealt with independently by effective rotational Hamiltonians related to the different vibrational states of the polyad.

Let $P_{n_1}^{\nu_{max}}$ be the set of indices n such that $0 \leq \nu_n - \nu_{n_1} \leq \nu_{max}$, $N_{\mathbf{x}}$ the cardinal of this set, and $n_{max} = n_{N_{\mathbf{x}}}$ be the largest element of this set,

$$P_{n_1}^{\nu_{max}} = \{n_1, n_1+1, \ldots, n_{max}-1, n_{max}\} \tag{6}$$

(the letter P is meant to evoque a "Polyad" of molecular spectroscopy which would contain the vibrational levels $n_1, \ldots, n_{max}$).
To solve perturbationally the eigenvalue equation,

$$H(X,Y)\phi = E\phi, \tag{7}$$

we introduce a real parameter, $\varepsilon \in [0,1]$, and the Hamiltonian,

$$H(X,Y,\varepsilon) = H_0(X) \otimes Id_{\mathbf{y}} + \varepsilon H_1(X,Y), \tag{8}$$

such that, $H(X,Y,0) = H_0(X) \otimes Id_{\mathbf{y}}$ and $H(X,Y,1) = H(X,Y)$.

So, for $\varepsilon = 0$,

$$H(X,Y,0)|\psi_i \otimes \Psi_K^i\rangle = \nu_i |\psi_i \otimes \Psi_K^i\rangle \quad \forall K, \tag{9}$$

showing that each eigenvalue ν_i is $(dimV_{\mathbf{y}})$-times degenerate (at least). Substituting $|\Psi_K^i\rangle_{\mathbf{y}}$ by $|\Psi_K^i\rangle_{\mathbf{y}} \cdot \langle \Psi_K^i|$ in $|\psi_i \otimes \Psi_K^i\rangle = |\psi_i\rangle_{\mathbf{x}} \otimes |\Psi_K^i\rangle_{\mathbf{y}}$ of Eq.(9), and summing over K, one obtains,

$$(H_0(X) \otimes Id_{\mathbf{y}})|\psi_i\rangle_{\mathbf{x}} \otimes Id_{\mathbf{y}} = \nu_i |\psi_i\rangle_{\mathbf{x}} \otimes Id_{\mathbf{y}}. \tag{10}$$

Assume that for a properly chosen set $P_{n_1}^{\nu_{max}}$, for all $\varepsilon \in [0,1]$, the $N_{\mathbf{x}} \times dimV_{\mathbf{y}}$ eigenstates $(\psi_{n_1} \otimes \Psi_K^{n_1})_K, \ldots, (\psi_{n_{max}} \otimes \Psi_K^{n_{max}})_K$ of $H(X,Y,0)$ can be related in a one-to-one correspondance to a set of $N_{\mathbf{x}} \times dimV_{\mathbf{y}}$ normalized eigenstates of $H(X,Y,\varepsilon)$, denoted by $(\phi_{j,K}(\varepsilon))_{j \leq N_{\mathbf{x}}, K \leq dimV_{\mathbf{y}}}$. The $\phi_{j,K}(\varepsilon)$'s can be expanded on the tensorial product basis set as,

$$\phi_{j,K}(\varepsilon) = \sum_{j',K'} c_{j',K'}^{j,K}(\varepsilon)\ \psi_{j'} \otimes \Psi_{K'}^{j'}, \tag{11}$$

(with no restriction on the summation on j' nor K').

Introducing the linear unitary operator, $\tilde{\Psi}(Y,\varepsilon)$, called the "effective wave superoperator", acting from the tensor space

$$\tilde{V}_{\mathbf{y}} := \bigoplus_{i=1}^{N_{\mathbf{x}}} \psi_{n_i} \otimes V_{\mathbf{y}}^{n_i} \tag{12}$$

(isomorphous to the Cartesian product vector space,$V_{\mathbf{y}}^{n_1} \times \cdots \times V_{\mathbf{y}}^{n_{max}}$), onto the linear span of the set $(\phi_{j,K}(\varepsilon))_{1 \leq j \leq N_{\mathbf{x}}, 1 \leq K \leq dimV_{\mathbf{y}}^n}$ and defined by

$$\forall i \leq N_{\mathbf{x}}, K_i \leq dimV_{\mathbf{y}}^{n_i}, \quad \tilde{\Psi}(Y,\varepsilon) \cdot \psi_{n_i} \otimes \Psi_{K_i}^{n_i} := \sum_{K',n'} c_{n',K'}^{n_i,K_i}(\varepsilon)\ \psi_{n'} \otimes \Psi_{K'}^{n'}, \tag{13}$$

The effective wave superoperator is the operator that sends the selected eigenfunctions of $H(X,Y,0)$ onto those of $H(X,Y,\varepsilon)$. We define another linear operator, $\tilde{E}(Y,\varepsilon)$, from

$\tilde{V}_{\mathbf{y}}$ onto $\tilde{V}_{\mathbf{y}}$, called the "effective superHamiltonian for $P_{n_1}^{\nu_{max}}$". It can be given explicitly by its action on the basis functions,

$$\tilde{E}(Y,\varepsilon)\cdot\Psi_{K_i}^{n_i} := E_{n_i,K_i}(\varepsilon)\Psi_{K_i}^{n_i}, \tag{14}$$

where $E_{i,K}(\varepsilon)$ denotes the eigenvalue associated to $\phi_{i,K}(\varepsilon)$, or equivalently by the equation

$$\tilde{E}(Y,\varepsilon) = \tilde{\Psi}(Y,\varepsilon)^\dagger \cdot H(X,Y,\varepsilon)\cdot\tilde{\Psi}(Y,\varepsilon), \tag{15}$$

which shows its Hermiticity. The latter equation can be rewritten formally as a generalized eigenproblem equation for an eigenpair of operators $\left(\tilde{E}(Y,\varepsilon),\tilde{\Psi}(Y,\varepsilon)\right)$,

$$H(X,Y,\varepsilon)\cdot\tilde{\Psi}(Y,\varepsilon) = \tilde{\Psi}(Y,\varepsilon)\cdot\tilde{E}(Y,\varepsilon). \tag{16}$$

For the case of interest, $\varepsilon = 1$, we alleviate the notation by ignoring the dependence upon ε,

$$H(X,Y)\cdot\tilde{\Psi}(Y) = \tilde{\Psi}(Y)\cdot\tilde{E}(Y). \tag{17}$$

Applying the operators of both members of Eq.(17) to any basis function,$\psi_{n_i}\otimes\Psi_K^{n_i}$, Eq.(7) is recovered for the eigenpair $(E_{n_i,K},\phi_{n_i,K})$ of $H(X,Y)$. The unitarity of the effective wave superoperator implies the normalization condition,

$$\tilde{\Psi}^\dagger(Y)\cdot\tilde{\Psi}(Y) = Id_{\tilde{V}_{\mathbf{y}}}, \tag{18}$$

where $Id_{\tilde{V}_{\mathbf{y}}}$ the identity on $\tilde{V}_{\mathbf{y}}$, can also be regarded as an effective operator associated to the identity operator on the total Hilbert space. More generally, effective operator for any observable can be obtained by using $\tilde{\Psi}(Y)$ to change the representation. Of prime importance for spectroscopy is the laboratory-fixed, dipole moment, $D(X,Y)$, acting on $V_{\mathbf{x}}\otimes V_{\mathbf{y}}$. Its effective counterpart, $\tilde{D}(Y)$, acting solely on $\tilde{V}_{\mathbf{y}}$, will be,

$$\tilde{D}(Y) = \tilde{\Psi}^\dagger(Y)\cdot D(X,Y)\cdot\tilde{\Psi}(Y). \tag{19}$$

B. Case of a symmetry operator $G(Y)$ commuting with $H(X,Y)$

Let us assume that a set of all commuting symmetry operators $(G_i(Y))_{i\in\{1,\cdots,p\}}$ commutes with $H(X,Y)$. Let us call J_i the eigenvalues of $G_i(Y)$, and decompose the Hilbert space $V_{\mathbf{y}}$ into the common eigenspaces of the $G_i(Y)$'s:

$$V_{\mathbf{y}} = \bigoplus_{J_1,\ldots,J_p} V_{\mathbf{y}}^{(J_1,\ldots,J_p)}. \tag{20}$$

In the case of the ro-vibrational problem, such symmetry operators will be the module of the total angular momentum and the z-component of the latter in the laboratory-fixed frame.

C. Generalized perturbation theory for the effective wave operator equation

In the previous section, we have shown that the "exact" effective wave superoperator and effective superHamiltonian were solutions of an "eigen equation" for operators, Eq. (16). (The prefix "super" is added because these operators act on n_{max} copies of subspaces of $V_{\mathbf{y}}$ and not just one, as in the non degenerate theory). However, at this stage, the unicity of the solution has not been established. In this section, we show how a Rayleigh-Schrödinger type of perturbational strategy permits to solve formally Eq. (16), and as a by-product, we obtain that this formal series is uniquely determined by a normalization and a phase condition.

We will look for the effective superoperators, $\tilde{\Psi}(Y,\varepsilon)$ and $\tilde{E}(Y,\varepsilon)$ that are analytical functions of ε:

$$\tilde{\Psi}(Y,\varepsilon) = \tilde{\Psi}^{(0)}(Y) + \varepsilon\tilde{\Psi}^{(1)}(Y) + \varepsilon^2\tilde{\Psi}^{(2)}(Y) + \varepsilon^3\tilde{\Psi}^{(3)}(Y) + \varepsilon^4\tilde{\Psi}^{(4)}(Y) + ..., \tag{21}$$

$$\tilde{E}(Y,\varepsilon) = \tilde{E}^{(0)}(Y) + \varepsilon\tilde{E}^{(1)}(Y) + \varepsilon^2\tilde{E}^{(2)}(Y) + \varepsilon^3\tilde{E}^{(3)}(Y) + \varepsilon^4\tilde{E}^{(4)}(Y) + ..., \tag{22}$$

with,

$$\tilde{\Psi}^{(0)}(Y) = \sum_{i\in P_{n_1}^{\nu_{max}}} |\psi_i\rangle_{\mathbf{x}}\langle\psi_i| \otimes Id_{V_{\mathbf{y}}^i} \tag{23}$$

$$\tilde{E}^{(0)}(Y) = \sum_{i\in P_{n_1}^{\nu_{max}}} \nu_i|\psi_i\rangle_{\mathbf{x}}\langle\psi_i| \otimes Id_{V_{\mathbf{y}}^i}. \tag{24}$$

Inserting these expressions in Eq. (16) and identifying the terms with the same power of ε, we obtain Eq.(10) for $k=0$, and for all $k>0$:

$$H_0(X)\otimes Id_{\mathbf{y}} \cdot \tilde{\Psi}^{(k)}(Y) + H_1(X,Y)\cdot\tilde{\Psi}^{(k-1)}(Y) = \sum_{i=0}^{k} \tilde{\Psi}^{(i)}(Y)\cdot\tilde{E}^{(k-i)}(Y). \tag{25}$$

Expressions of $\tilde{E}^{(k)}(Y)$ and $\tilde{\Psi}^{(k)}(Y)$ for $k>0$ are derived below by enforcing the set of normalization conditions, $\forall k>0$,

$$\left(\sum_{i=0}^{k}\varepsilon^i\tilde{\Psi}^{(i)\dagger}(Y)\right)\cdot\left(\sum_{i=0}^{k}\varepsilon^i\tilde{\Psi}^{(i)}(Y)\right) = Id_{\tilde{V}_{\mathbf{y}}} + o(\varepsilon^k, Y), \tag{26}$$

where the notation $o(\varepsilon^k,Y)$ means that $\lim_{\varepsilon\to 0}\varepsilon^{-k}o(\varepsilon^k,Y) = 0_{\tilde{V}_{\mathbf{y}}}$, the null operator on $\tilde{V}_{\mathbf{y}}$, and the set of "Hermiticity" conditions (as operators restricted to $\tilde{V}_{\mathbf{y}}$):
$\forall i,j \in P_{n_1}^{\nu_{max}}, k>0$,

$$\langle\psi_i\otimes Id_{V_{\mathbf{y}}^i}|\tilde{\Psi}^{(k)}(Y)|\psi_j\otimes Id_{V_{\mathbf{y}}^j}\rangle_{\mathbf{x}} = \langle\psi_i\otimes Id_{V_{\mathbf{y}}^i}|\tilde{\Psi}^{(k)\dagger}(Y)|\psi_j\otimes Id_{V_{\mathbf{y}}^j}\rangle_{\mathbf{x}}. \tag{27}$$

Here the notation $\langle\cdots\rangle_{\mathbf{x}}$ generalizes that of kets of $V_{\mathbf{x}}$ and means that integration is carried over the $\mathbf{x}$-variables only, for example,

$$\langle\psi_1\otimes\Psi_1(Y)|\psi_2\otimes\Psi_2(Y)\rangle_{\mathbf{x}}=\langle\psi_1|\psi_2\rangle_{\mathbf{x}}\Psi_1(Y)\Psi_2(Y). \tag{28}$$

These conditions are to some extend arbitrary, however they are the natural ones to impose in view of computing effective observables that are properly normalized and to have effective superoperator first order corrections that cancel out on the effective Hilbert space $\tilde{V}_{\mathbf{y}}$.

1. First order:

For $k=1$, Eq. (25) becomes

$$\begin{aligned}&H_0(X)\otimes Id_{\mathbf{y}}\cdot\tilde{\Psi}^{(1)}(Y)+H_1(X,Y)\cdot\sum_{i\in P_{n_1}^{\nu_{max}}}|\psi_i\rangle_{\mathbf{x}}\langle\psi_i|\otimes Id_{V_{\mathbf{y}}^i}\\&=\tilde{\Psi}^{(1)}(Y)\cdot\sum_{i\in P_{n_1}^{\nu_{max}}}\nu_i\;|\psi_i\rangle_{\mathbf{x}}\langle\psi_i|\otimes Id_{V_{\mathbf{y}}^i}+\sum_{i\in P_{n_1}^{\nu_{max}}}|\psi_i\rangle_{\mathbf{x}}\langle\psi_i|\otimes Id_{V_{\mathbf{y}}^i}\cdot\tilde{E}^{(1)}(Y).\end{aligned} \tag{29}$$

Multiplying by $\langle\psi_i\otimes Id_{V_{\mathbf{y}}^i}|$ on the left and by $|\psi_j\otimes Id_{V_{\mathbf{y}}^j}\rangle$ on the right, $i,j\in P_{n_1}^{\nu_{max}}$, we obtain

$$\langle\psi_i\otimes Id_{V_{\mathbf{y}}^i}|\tilde{E}^{(1)}(Y)|\psi_j\otimes Id_{V_{\mathbf{y}}^j}\rangle_{\mathbf{x}}=\langle\psi_i\otimes Id_{V_{\mathbf{y}}^i}|H_1(X,Y)|\psi_j\otimes Id_{V_{\mathbf{y}}^j}\rangle_{\mathbf{x}}. \tag{30}$$

This equation determines the action of $\tilde{E}^{(1)}(Y)$ as an operator from $\tilde{V}_{\mathbf{y}}$ onto $\tilde{V}_{\mathbf{y}}$.

Making use of Eqs (26) and (27) for $k=1$, we get,

$$\langle\psi_i\otimes Id_{V_{\mathbf{y}}^i}|\tilde{\Psi}^{(1)}(Y)|\psi_j\otimes Id_{V_{\mathbf{y}}^j}\rangle_{\mathbf{x}}=0_{V_{\mathbf{y}}^j}, \tag{31}$$

the null operator on $V_{\mathbf{y}}^j$.

Projecting Eq.(29) onto $\langle\psi_{k_1}\otimes Id_{V^{k_1}}|$, for $k_1\notin P_{n_1}^{\nu_{max}}$, on the left and onto $|\psi_j\otimes Id_{V^j}\rangle$, for $j\in P_{n_1}^{\nu_{max}}$, on the right, we obtain

$$\langle\psi_{k_1}\otimes Id_{V_{\mathbf{y}}^{k_1}}|\tilde{\Psi}^{(1)}(Y)|\psi_j\otimes Id_{V_{\mathbf{y}}^j}\rangle_{\mathbf{x}}=\frac{\langle\psi_{k_1}\otimes Id_{V_{\mathbf{y}}^{k_1}}|H_1(X,Y)|\psi_j\otimes Id_{V_{\mathbf{y}}^j}\rangle_{\mathbf{x}}}{\nu_j-\nu_{k_1}}. \tag{32}$$

Equations (31) and (32) completely determine the action of $\tilde{\Psi}^{(1)}(Y)$ on $\tilde{V}_{\mathbf{y}}$.

In the following, we will use the compact notation,

$$H_1(Y)_{i,j}:=\langle\psi_i\otimes Id_{V_{\mathbf{y}}^i}|H_1(X,Y)|\psi_j\otimes Id_{V_{\mathbf{y}}^j}\rangle_{\mathbf{x}}, \tag{33}$$

so that,

$$\tilde{E}^{(1)}(Y)=\sum_{i,j\in P_{n_1}^{\nu_{max}}}H_1(Y)_{i,j}\cdot|\psi_i\otimes Id_{V_{\mathbf{y}}^i}\rangle\langle\psi_j\otimes Id_{V_{\mathbf{y}}^j}|, \tag{34}$$

and

$$\tilde{\Psi}^{(1)}(Y)=\sum_{k_1\notin P_{n_1}^{\nu_{max}},j\in P_{n_1}^{\nu_{max}}}\frac{H_1(Y)_{k_1,j}}{\nu_j-\nu_{k_1}}\cdot|\psi_{k_1}\otimes Id_{V_{\mathbf{y}}^{k_1}}\rangle\langle\psi_j\otimes Id_{V_{\mathbf{y}}^j}|, \tag{35}$$

2. *Second order*

Using the normalization and Hermiticity conditions (Eqs (26) and (27) for $k = 2$), and the Hermiticity of $H_1(X, Y)$ (as an operator acting on V), we obtain

$$\langle \psi_i \otimes Id_{V_{\mathbf{y}}^i} | \tilde{\Psi}^{(2)}(Y) | \psi_j \otimes Id_{V_{\mathbf{y}}^j} \rangle_{\mathbf{x}} = -\tfrac{1}{2} \sum_{k_1 \notin P_{n_1}^{\nu_{max}}} \frac{H_1(Y)_{i,k_1} H_1(Y)_{k_1,j}}{(\nu_i - \nu_{k_1})(\nu_j - \nu_{k_1})}. \tag{36}$$

For $k = 2$, Eq. (25) becomes

$$\begin{aligned} H_0(X) \otimes Id_{\mathbf{y}} \cdot \tilde{\Psi}^{(2)}(Y) + H_1(X,Y) \cdot \sum_{k_1 \notin P_{n_1}^{\nu_{max}}, l_1 \in P_{n_1}^{\nu_{max}}} \frac{H_1(Y)_{k_1,l_1}}{\nu_{l_1} - \nu_{k_1}} \cdot |\psi_{k_1} \otimes Id_{V_{\mathbf{y}}^{k_1}}\rangle\langle \psi_{l_1} \otimes Id_{V_{\mathbf{y}}^{l_1}}| \\ = \sum_{l_1 \in P_{n_1}^{\nu_{max}}} |\psi_{l_1}\rangle_{\mathbf{x}}\langle\psi_{l_1}| \otimes Id_{V_{\mathbf{y}}^{l_1}} \cdot \tilde{E}^{(2)}(Y) \\ + \sum_{k_1 \notin P_{n_1}^{\nu_{max}}; l_1, l_2 \in P_{n_1}^{\nu_{max}}} \frac{H_1(Y)_{k_1,l_1} H_1(Y)_{l_1,l_2}}{\nu_{l_1} - \nu_{k_1}} \cdot |\psi_{k_1} \otimes Id_{V_{\mathbf{y}}^{k_1}}\rangle\langle \psi_{l_2} \otimes Id_{V_{\mathbf{y}}^{l_2}}| \\ + \tilde{\Psi}^{(2)}(Y) \cdot \sum_{l_1 \in P_{n_1}^{\nu_{max}}} \nu_{l_1} \ |\psi_{l_1}\rangle_{\mathbf{x}}\langle\psi_{l_1}| \otimes Id_{V_{\mathbf{y}}^{l_1}}. \end{aligned} \tag{37}$$

Projecting Eq.(29) onto $\langle \psi_i \otimes Id_{V_{\mathbf{y}}^i}|$ on the left and onto $|\psi_j \otimes Id_{V_{\mathbf{y}}^j}\rangle$ on the right, for $i, j \in P_{n_1}^{\nu_{max}}$, and using Eq.(36), we obtain

$$\langle \psi_i \otimes Id_{V_{\mathbf{y}}^i} | \tilde{E}^{(2)}(Y) | \psi_j \otimes Id_{V_{\mathbf{y}}^j} \rangle_{\mathbf{x}} = \tfrac{1}{2} \sum_{k_1 \notin P_{n_1}^{\nu_{max}}} H_1(Y)_{i,k_1} H_1(Y)_{k_1,j} \left(\frac{1}{\nu_i - \nu_{k_1}} + \frac{1}{\nu_j - \nu_{k_1}} \right), \tag{38}$$

which determines $\tilde{E}^{(2)}$. Projecting Eq.(37) onto $\langle \psi_{k_2} \otimes Id_{V^{k_2}}|$ on the left and onto $|\psi_j \otimes Id_{V^j}\rangle$ on the right, for $k_2 \notin P_{n_1}^{\nu_{max}}, j \in P_{n_1}^{\nu_{max}}$, we obtain

$$\langle \psi_{k_2} \otimes Id_{V_{\mathbf{y}}^{k_2}} | \tilde{\Psi}^{(2)}(Y) | \psi_j \otimes Id_{V_{\mathbf{y}}^j} \rangle_{\mathbf{x}} = \sum_{k_1 \notin P_{n_1}^{\nu_{max}}} \frac{H_1(Y)_{k_2,k_1} H_1(Y)_{k_1,j}}{(\nu_j - \nu_{k_1})(\nu_j - \nu_{k_2})} - \sum_{l_1 \in P_{n_1}^{\nu_{max}}} \frac{H_1(Y)_{k_2,l_1} H_1(Y)_{l_1,j}}{(\nu_{l_1} - \nu_{k_2})(\nu_j - \nu_{k_2})}. \tag{39}$$

Equations (39) and (36) determine $\tilde{\Psi}^{(2)}$.

3. *Higher orders*

We proceeds as for the second order and obtain after some tedious but straightforward algebra, at order 3, for $i, j \in P_{n_1}^{\nu_{max}}$

$$\begin{aligned} \langle \psi_i \otimes Id_{V_{\mathbf{y}}^i} | \tilde{\Psi}^{(3)}(Y) | \psi_j \otimes Id_{V_{\mathbf{y}}^j} \rangle_{\mathbf{x}} = \\ - \tfrac{1}{2} \sum_{k_1, k_2 \notin P_{n_1}^{\nu_{max}}} \frac{H_1(Y)_{i,k_1} H_1(Y)_{k_1,k_2} H_1(Y)_{k_2,j}}{(\nu_i - \nu_{k_1})(\nu_j - \nu_{k_2})} \left(\frac{1}{\nu_i - \nu_{k_2}} + \frac{1}{\nu_j - \nu_{k_1}} \right) \\ + \tfrac{1}{2} \sum_{k_1 \notin P_{n_1}^{\nu_{max}}, l_1 \in P_{n_1}^{\nu_{max}}} \frac{H_1(Y)_{i,l_1} H_1(Y)_{l_1,k_1} H_1(Y)_{k_1,j} + H_1(Y)_{i,k_1} H_1(Y)_{k_1,l_1} H_1(Y)_{l_1,j}}{(\nu_i - \nu_{k_1})(\nu_j - \nu_{k_1})(\nu_{l_1} - \nu_{k_1})}, \end{aligned} \tag{40}$$

$$
\begin{aligned}
&\langle \psi_i \otimes Id_{V_{\mathbf{y}}^i} | \tilde{E}^{(3)}(Y) | \psi_j \otimes Id_{V_{\mathbf{y}}^j} \rangle_{\mathbf{x}} \\
&= \tfrac{1}{2} \sum_{k_1,k_2 \notin P_{n_1}^{\nu max}} H_1(Y)_{i,k_1} H_1(Y)_{k_1,k_2} H_1(Y)_{k_2,j} \left(\tfrac{1}{(\nu_i - \nu_{k_1})(\nu_i - \nu_{k_2})} + \tfrac{1}{(\nu_j - \nu_{k_1})(\nu_j - \nu_{k_2})} \right) \\
&\quad - \tfrac{1}{2} \sum_{k_1 \notin P_{n_1}^{\nu max}, l_1 \in P_{n_1}^{\nu max}} \frac{H_1(Y)_{i,k_1} H_1(Y)_{k_1,l_1} H_1(Y)_{l_1,j}}{(\nu_{l_1} - \nu_{k_1})(\nu_j - \nu_{k_1})} + \frac{H_1(Y)_{i,l_1} H_1(Y)_{l_1,k_1} H_1(Y)_{k_1,j}}{(\nu_i - \nu_{k_1})(\nu_{l_1} - \nu_{k_1})}.
\end{aligned}
\tag{41}
$$

For $k_1 \notin P_{n_1}^{\nu_{max}}, j \in P_{n_1}^{\nu_{max}}$

$$
\begin{aligned}
&\langle \psi_{k_1} \otimes Id_{V_{\mathbf{y}}^{k_1}} | \tilde{\Psi}^{(3)}(Y) | \psi_j \otimes Id_{V_{\mathbf{y}}^j} \rangle_{\mathbf{x}} = \sum_{k_2,k_3 \notin P_{n_1}^{\nu max}} \frac{H_1(Y)_{k_1,k_2} H_1(Y)_{k_2,k_3} H_1(Y)_{k_3,j}}{(\nu_j - \nu_{k_1})(\nu_j - \nu_{k_2})(\nu_j - \nu_{k_3})} \\
&\sum_{l_1,l_2 \in P_{n_1}^{\nu max}} \frac{H_1(Y)_{k_1,l_1} H_1(Y)_{l_1,l_2} H_1(Y)_{l_2,j}}{(\nu_j - \nu_{k_1})(\nu_{l_1} - \nu_{k_1})(\nu_{l_2} - \nu_{k_1})} - \sum_{l_1 \in P_{n_1}^{\nu max}, k_2 \notin P_{n_1}^{\nu max}} \frac{H_1(Y)_{k_1,k_2} H_1(Y)_{k_2,l_1} H_1(Y)_{l_1,j}}{(\nu_j - \nu_{k_1})(\nu_{l_1} - \nu_{k_2})} \left(\frac{1}{(\nu_j - \nu_{k_2})} + \frac{1}{(\nu_{l_1} - \nu_{k_1})} \right) \\
&- \tfrac{1}{2} \sum_{l_1 \in P_{n_1}^{\nu max}, k_2 \notin P_{n_1}^{\nu max}} \frac{H_1(Y)_{k_1,l_1} H_1(Y)_{l_1,k_2} H_1(Y)_{k_2,j}}{(\nu_j - \nu_{k_1})} \left(\frac{1}{(\nu_{l_1} - \nu_{k_2})(\nu_j - \nu_{k_2})} + \frac{1}{(\nu_{l_1} - \nu_{k_1})(\nu_{l_1} - \nu_{k_2})} + \frac{1}{(\nu_{l_1} - \nu_{k_1})(\nu_j - \nu_{k_2})} \right).
\end{aligned}
\tag{42}
$$

Then, at order 4, for $i, j \in P_{n_1}^{\nu_{max}}$

$$
\begin{aligned}
&\langle \psi_i \otimes Id_{V_{\mathbf{y}}^i} | \tilde{\Psi}^{(4)}(Y) | \psi_j \otimes Id_{V_{\mathbf{y}}^j} \rangle_{\mathbf{x}} = \\
&- \tfrac{1}{2} \sum_{k_1,k_2,k_3 \notin P_{n_1}^{\nu max}} \frac{H_1(Y)_{i,k_1} H_1(Y)_{k_1,k_2} H_1(Y)_{k_2,k_3} H_1(Y)_{k_3,j}}{(\nu_i - \nu_{k_1})(\nu_j - \nu_{k_3})} \left(\tfrac{1}{(\nu_j - \nu_{k_1})(\nu_j - \nu_{k_2})} + \tfrac{1}{(\nu_i - \nu_{k_2})(\nu_j - \nu_{k_2})} + \tfrac{1}{(\nu_i - \nu_{k_2})(\nu_i - \nu_{k_3})} \right) \\
&+ \tfrac{1}{2} \sum_{k_1,k_2 \notin P_{n_1}^{\nu max}, l_1 \in P_{n_1}^{\nu max}} \frac{H_1(Y)_{i,k_1} H_1(Y)_{k_1,l_1} H_1(Y)_{l_1,k_2} H_1(Y)_{k_2,j}}{(\nu_i - \nu_{k_1})(\nu_j - \nu_{k_2})} \left(\tfrac{3}{4(\nu_{l_1} - \nu_{k_1})(\nu_{l_1} - \nu_{k_2})} + \tfrac{1}{(\nu_i - \nu_{k_2})(\nu_{l_1} - \nu_{k_2})} + \tfrac{1}{(\nu_j - \nu_{k_1})(\nu_{l_1} - \nu_{k_1})} \right) \\
&+ \tfrac{1}{2} \sum_{k_1,k_2 \notin P_{n_1}^{\nu max}, l_1 \in P_{n_1}^{\nu max}} \frac{H_1(Y)_{i,k_1} H_1(Y)_{k_1,k_2} H_1(Y)_{k_2,l_1} H_1(Y)_{l_1,j}}{(\nu_i - \nu_{k_1})(\nu_{l_1} - \nu_{k_2})} \left(\tfrac{1}{(\nu_i - \nu_{k_2})(\nu_j - \nu_{k_2})} + \tfrac{1}{(\nu_j - \nu_{k_1})(\nu_j - \nu_{k_2})} + \tfrac{1}{(\nu_{l_1} - \nu_{k_1})(\nu_j - \nu_{k_1})} \right) \\
&+ \tfrac{1}{2} \sum_{k_1,k_2 \notin P_{n_1}^{\nu max}, l_1 \in P_{n_1}^{\nu max}} \frac{H_1(Y)_{i,l_1} H_1(Y)_{l_1,k_1} H_1(Y)_{k_1,k_2} H_1(Y)_{k_2,j}}{(\nu_j - \nu_{k_2})(\nu_{l_1} - \nu_{k_1})} \left(\tfrac{1}{(\nu_i - \nu_{k_1})(\nu_j - \nu_{k_1})} + \tfrac{1}{(\nu_i - \nu_{k_1})(\nu_i - \nu_{k_2})} + \tfrac{1}{(\nu_i - \nu_{k_2})(\nu_{l_1} - \nu_{k_2})} \right) \\
&- \tfrac{1}{2} \sum_{k_1 \notin P_{n_1}^{\nu max}, l_1, l_2 \in P_{n_1}^{\nu max}} \frac{H_1(Y)_{i,l_1} H_1(Y)_{l_1,k_1} H_1(Y)_{k_1,l_2} H_1(Y)_{l_2,j} + H_1(Y)_{i,k_1} H_1(Y)_{k_1,l_1} H_1(Y)_{l_1,l_2} H_1(Y)_{l_2,j} + H_1(Y)_{i,l_1} H_1(Y)_{l_1,l_2} H_1(Y)_{l_2,k_1} H_1(Y)_{k_1,j}}{(\nu_i - \nu_{k_1})(\nu_j - \nu_{k_1})(\nu_{l_1} - \nu_{k_1})(\nu_{l_2} - \nu_{k_1})},
\end{aligned}
\tag{43}
$$

$$
\begin{aligned}
&\langle \psi_i \otimes Id_{V_{\mathbf{y}}^i} | \tilde{E}^{(4)}(Y) | \psi_j \otimes Id_{V_{\mathbf{y}}^j} \rangle_{\mathbf{x}} = \\
&\tfrac{1}{2} \sum_{k_1,k_2,k_3 \notin P_{n_1}^{\nu max}} H_1(Y)_{i,k_1} H_1(Y)_{k_1,k_2} H_1(Y)_{k_2,k_3} H_1(Y)_{k_3,j} \left(\tfrac{1}{(\nu_i - \nu_{k_1})(\nu_i - \nu_{k_2})(\nu_i - \nu_{k_3})} + \tfrac{1}{(\nu_j - \nu_{k_1})(\nu_j - \nu_{k_2})(\nu_j - \nu_{k_3})} \right) \\
&- \tfrac{1}{2} \sum_{k_1,k_2 \notin P_{n_1}^{\nu max}, l_1 \in P_{n_1}^{\nu max}} H_1(Y)_{i,k_1} H_1(Y)_{k_1,l_1} H_1(Y)_{l_1,k_2} H_1(Y)_{k_2,j} \left(\tfrac{1}{4(\nu_{l_1} - \nu_{k_1})(\nu_{l_1} - \nu_{k_2})} \left(\tfrac{1}{\nu_i - \nu_{k_1}} + \tfrac{1}{\nu_j - \nu_{k_2}} \right) \right. \\
&\quad - \tfrac{1}{4(\nu_i - \nu_{k_1})(\nu_j - \nu_{k_2})} \left(\tfrac{1}{\nu_{l_1} - \nu_{k_1}} + \tfrac{1}{\nu_{l_1} - \nu_{k_2}} \right) + \left. \tfrac{1}{(\nu_i - \nu_{k_1})(\nu_i - \nu_{k_2})(\nu_{l_1} - \nu_{k_2})} + \tfrac{1}{(\nu_j - \nu_{k_1})(\nu_j - \nu_{k_2})(\nu_{l_1} - \nu_{k_1})} \right) \\
&\quad - \tfrac{1}{2} \sum_{k_1,k_2 \notin P_{n_1}^{\nu max}, l_1 \in P_{n_1}^{\nu max}} \frac{H_1(Y)_{i,k_1} H_1(Y)_{k_1,k_2} H_1(Y)_{k_2,l_1} H_1(Y)_{l_1,j}}{(\nu_{l_1} - \nu_{k_2})(\nu_j - \nu_{k_1})} \left(\tfrac{1}{\nu_j - \nu_{k_2}} + \tfrac{1}{\nu_{l_1} - \nu_{k_1}} \right) \\
&\quad - \tfrac{1}{2} \sum_{k_1,k_2 \notin P_{n_1}^{\nu max}, l_1 \in P_{n_1}^{\nu max}} \frac{H_1(Y)_{i,l_1} H_1(Y)_{l_1,k_1} H_1(Y)_{k_1,k_2} H_1(Y)_{k_2,j}}{(\nu_i - \nu_{k_2})(\nu_{l_1} - \nu_{k_1})} \left(\tfrac{1}{\nu_i - \nu_{k_1}} + \tfrac{1}{\nu_{l_1} - \nu_{k_2}} \right) \\
&\tfrac{1}{2} \sum_{k_1 \notin P_{n_1}^{\nu max}, l_1, l_2 \in P_{n_1}^{\nu max}} \left(\frac{H_1(Y)_{i,l_1} H_1(Y)_{l_1,l_2} H_1(Y)_{l_2,k_1} H_1(Y)_{k_1,j}}{(\nu_i - \nu_{k_1})(\nu_{l_1} - \nu_{k_1})(\nu_{l_2} - \nu_{k_1})} + \frac{H_1(Y)_{i,k_1} H_1(Y)_{k_1,l_1} H_1(Y)_{l_1,l_2} H_1(Y)_{l_2,j}}{(\nu_j - \nu_{k_1})(\nu_{l_1} - \nu_{k_1})(\nu_{l_2} - \nu_{k_1})} \right).
\end{aligned}
\tag{44}
$$

So the perturbative solution to Eq.(17) is actually unique at all orders for a given H, within the normalization and Hermiticity constraints. Of course, if H is transformed by

a unitary mapping, the effective wave superoperator and effective superHamiltonian will be transformed accordingly.

Remark 1: Equations (38), (41) and (44), reduce to the non degenerate formulas of our previous work, see[42]. However, they are more involved than the classical formulas for the quasi-degenerate case reported in textbooks, which consist at second order for example, in substituting the quasi-degenerate eigenvalues by their barycentric mean: $\nu_i, \nu_j \rightarrow \nu^{barycentric} = \sum_{l \in P_{n_1}^{\nu max}} \frac{\nu_l}{N_{\mathbf{x}}}$, or by their arithmetic mean: $\nu_i, \nu_j \rightarrow \nu_{i,j}^{arithmetic} = \frac{\nu_i + \nu_j}{2}$. The first case has the advantage that $\nu^{barycentric}$ is independent from i and j,

$$\langle \psi_i \otimes Id_{V_{\mathbf{y}}^i} | \tilde{E}^{(2)}(Y) | \psi_j \otimes Id_{V_{\mathbf{y}}^j} \rangle_{\mathbf{x}} = \sum_{k_1 \notin P_{n_1}^{\nu max}} \frac{H_1(Y)_{i,k_1} H_1(Y)_{k_1,j}}{\nu^{barycentric} - \nu_{k_1}}. \tag{45}$$

However, the convergence of the series is really poor as one departs from exact degeneracy. The "arithmetic mean denominator" ansatz

$$\langle \psi_i \otimes Id_{V_{\mathbf{y}}^i} | \tilde{E}^{(2)}(Y) | \psi_j \otimes Id_{V_{\mathbf{y}}^j} \rangle_{\mathbf{x}} = \sum_{k_1 \notin P_{n_1}^{\nu max}} \frac{H_1(Y)_{i,k_1} H_1(Y)_{k_1,j}}{\nu_{i,j}^{arithmetic} - \nu_{k_1}}, \tag{46}$$

performs better (see ref.[43]). However, this *ad hoc* ansatz is not as satisfactory as the harmonic mean: $\frac{1}{2}\left(\frac{1}{\nu_i - \nu_{k_1}} + \frac{1}{\nu_j - \nu_{k_1}}\right)$ that comes out from the generalized Rayleigh-Schrödinger method, and does not perform better for the cases studied so far.

Remark 2: Equations (38), (41) and (44) are exactly equivalent to those of Appendix B of Ref.[44], however, our expression for order 4 is slightly more compact.

II. APPLICATION TO THE TETRADECADE OF METHANE

To assess our generalized quasi-degenerate perturbation theory, and study the interplay between the choice of the quasi-degenerate space and the order of perturbation, we have chosen to focus on the $2\nu_3$-band of the tetradecade of methane. The methane ro-vibrational spectrum is decomposed into polyads corresponding to the approximate quantum number $P = 2n_1 + n_2 + 2n_3 + n_4$, where n_1 is the (approximate) number of quanta in the totally symmetric A_1 stretching mode ν_1, n_2 is the number of quanta in the doubly degenerate bending mode ν_2 of E symmetry, n_3 corresponds to the antisymmetric stretching mode ν_3 of F_2-symmetry, and n_4 to the bending mode ν_4 of F_2-symmetry. The n_i being non-negative integers, there are 14 different ways to make

up $P = 4$, hence the name "tetradecad" for this polyad. The $2\nu_3$-band, corresponds to $n_1 = n_2 = n_4 = 0, n_3 = 2$, so is one of the 14 possibilities.

A. Vibrational (J=0)-calculations

The implementation of the perturbation method supposes that the zero order problem has been solved. So, we first describe how the zero-order, that is to say, the vibrational (J=0)-Hamiltonian eigenproblem has been dealt with.

The potential energy surface (PES) has been derived from that of Nikitin-Rey-Tuyterev (NRT) PES[45]: First the latter has been expanded up to the 14^{th} order in Cartesian normal coordinates. Then, it has been converted to an expansion in terms of creation and annihilation operators and truncated at sixth order. Finally, it has been transformed back to Cartesian normal coordinates. This process allows one to obtain compact PES expression of lower order while (i) preserving a very good accuracy and (ii) avoiding spurious minima specific to standard high-order polynomial Taylor expansions[46]. The Watson μ-matrix has been treated similarly with an initial expansion in normal coordinates up to 8^{th} order.

Each modal basis set has been optimized by using a maximum overlap criterium with respect to a fixed number, p, of eigenstates of the Hamiltonian averaged over the other modes in their approximate harmonic ground state. These reference eigenfunctions and corresponding eigenvalues are denoted by $\{\psi_m\}_{m\in\{0,\ldots,p\}}$ and $\{\lambda_m\}_{m\in\{0,\ldots,p\}}$, where $m = 0$ corresponds to the ground state, $m = 1$ to the first excited state and so on. They are supposed to be known with sufficient accuracy. Let $\{\phi_m(\alpha_1, \cdots, \alpha_l)\}_{m\in\{0,\ldots,d\}}$ $(d \geq p)$ be a d-dimensional basis set made of eigenfunctions of a model potential depending on parameters, $(\alpha_1, \cdots, \alpha_l)$. In the vector space spanned by this basis set, the same mean field Hamiltonian has approximate eigenfunctions and eigenvalues denoted by $\{\tilde{\psi}_m(\alpha_1, \cdots, \alpha_l)\}_{m\in\{0,\ldots,p\}}$ and $\{\tilde{\lambda}_m(\alpha_1, \cdots, \alpha_l)\}_{m\in\{0,\ldots,p\}}$ with $\tilde{\psi}_m(\alpha_1, \cdots, \alpha_l) = \sum_{k=1}^{d} a_{mk}\phi_k(\alpha_1, \cdots, \alpha_l)$ and $\sum_{k=1}^{d} |a_{mk}|^2 = 1$. The optimal parameters are derived by maximising the quantity $\sum_{m=1}^{p} \underset{1\leq k\leq d}{sup} (|a_{mk}(\alpha_1, \cdots, \alpha_l)|^2)$ in the case of a non-degenerate mode, or its generalization $\sum_{m=1}^{p} \underset{K}{sup}(\sum_{k_i\in K} |a_{mk_i}(\alpha_1, \cdots, \alpha_l)|^2)$ where each K gathers the indices of a set of degenerate basis function. An additional constraint on the eigenvalues of the type $\max_{m\leq p}(|\tilde{\lambda}_m(\alpha_1, \cdots, \alpha_l) - \lambda_m|) < \varepsilon$ for a given ε can be also considered. In practice, the NRT PES reexpanded only to 10^{th} order in Cartesian normal coordinates and transformed to a sixth order expansion was used for the optimization. The ref-

erence $\{\psi_m\}_{m\in\{0,\ldots,p\}}$ and $\{\lambda_m\}_{m\in\{0,\ldots,p\}}$ were obtained by diagonalizing the mean field Hamiltonian in a large basis (dimension larger than d, typically up to quantum number equal to 20). The parameter p was adjusted for each mode so as to include all eigenvalues below the gap located in the range $23100 - 24300$ cm^{-1} , depending upon the mode. For modes 1 and 2, the constraint on eigenvalues was considered with $\varepsilon = 10^{-2}$ (given the accuracy of the PES), but it was found transparent for parameter sets such that $\sum_{m=1}^{p} \underset{K}{sup}(\sum_{k_i\in K} |a_{mk_i}(\alpha_1,\cdots,\alpha_l)|^2) \approx p$. (Note that achieving such large values for the overlap is not always possible when p is close to d). For stretching modes the maximal sum of quantum numbers of product basis functions was 14 and for bending modes, it was 16. So, the dimensions of the basis sets used were $d+1 = 15$ for ν_1, $d+1 = \binom{17+2-1}{2} = 153$ for ν_2, $d+1 = \binom{15+3-1}{3} = 680$ for ν_3, and $d = \binom{17+3-1}{3} = 969$ for ν_4. The optimized modal basis functions for mode 1 were eigenfunctions of a Kratzer potential[47,48], $D\left(\frac{Q}{Q+a}\right)^2$, with parameters ($D = 278500$ cm^{-1} , $a = 113.75$ au), Q mass-weighted coordinate. The projection criterium was 5.933 for $p = 6$. This was better than what could be obtained with a shift and frequency optimized Harmonic oscillator. For the other modes, they were eigenfunctions of harmonic oscillator potentials with respective wave numbers equal to 1510 cm^{-1} , 3150 cm^{-1} , and 1310 cm^{-1} for modes 2, 3 and 4. The projection criterium was 53.932 for $p = 55$ (resp. 31.427 for $p = 35$, and 261.406 for $p = 286$) for these three modes.

The $9D$ ($J = 0$)-Vibrational Hamiltonian was diagonalized with the vibrational mean field configuration interaction (VMFCI) method as implemented in the CONVIV code[2,49,50]. The contraction-truncation scheme was in our notation:
MSP-VSCFCI/VSCFCI($\nu_1-\nu_3$,$\nu_2-\nu_4$; 32615, 16851)/VCI(0,9343; 27535), in which:
- MSP-VSCFCI stands for minimal symmetry preserving (MSP) vibrational self-consistent configuration interaction calculation (VSCFCI). It means that the DOFs pertaining to the same degenerate mode have been contracted together in the mean field of the other DOFs and that this partition has been iterated until self-consistency was achieved.
- VSCFCI($\nu_1-\nu_3$,$\nu_2-\nu_4$; 32615, 16851) means that the stretching modes 1 and 3 are contracted with truncation of the product basis functions at 32615 cm^{-1} on the sum of the energies of their components, that the bending modes 2 and 4 are contracted with truncation of the product basis functions at 16851 cm^{-1} on the sum of the energies of their components, and that self-consistency was achieved for this new partition. The truncation thresholds have been chosen to fall in gaps of the spectra.
- VCI(0,9343; 27535) denotes as usual a vibrational configuration interaction (VCI)

step where the product basis set made of stretching and bending effective Hamiltonian eigenfunctions were truncated at 9343 cm^{-1} for the bending and at 27535 cm^{-1} on the sum of the stretching and bending energies. (Here again these values were chosen to fall in gaps of the spectra). The resulting size of the Hamiltonian matrix was 133646. The energy levels up to the tetradecad are given as supplementary material.

B. Reference variational calculation

A large variational calculation for the same Hamiltonian was performed by using the TENSOR computer code developed in Reims. This code is able to make use of the T_d symmetry of the system combined with irreducible tensor operators, and therefore to reduce the computational effort by a factor 10.

First, the vibrational ($J = 0$)-Hamiltonian was diagonalized in a harmonic oscillator product basis set $F(13)$ including all products such that the sum of quantum numbers was less or equal to 13. The frequencies of the modals were the fundamental harmonic frequencies of the Hamiltonian after transformation. The ($J = 0$)-spectrum is given as supplementary material up to the tetradecad. Although, the differences with the VMFCI results are small (RMS of 0.385 cm^{-1} , zero point energy (ZPE) of 9703.172 cm^{-1} was converged to better than the thousandth of cm^{-1}), these reference values (up to the tetradecad, only) were used to shift the band centers in the pertubative calculations of the following sections for a better comparison of rotational levels. For the $2\nu_3$ band of interest in this study, the shift is only of a few hundredth of cm^{-1} .

For $J > 0$, a set of rovibrational basis functions is built as the tensor product between the vibrational functions $\otimes_{i=1}^{4}\phi_i^{(C_{vi})}$ and symmetry-adapted rotational functions $\mid J, nC\sigma\rangle = \sum_m {}^{(J)}G^m_{nC\sigma} \mid J, m\rangle$, where the orientation matrix G is given in[51]. However the size of the rovibrational basis becomes intractable when using the vibrational $F(13)$ functions. Then, a compact set of orthonormalized vibrational ($J = 0$)-eigenvectors has been selected up to $F(7)$. These so-called reduced functions[25,52] were directly used to build a direct product ro-vibrational basis set and diagonalize the full Hamiltonian for $J \neq 0$. The so-obtained reference energy levels are estimated to be converged to the hundredth of cm^{-1} or better. They are given for the $2\nu_3$ band as supplementary material.

C. Quasi-degenerate pertubative calculations

The quasi-degenerate pertubative formulas of section I have been implemented up to fourth order for quasi-degenerate spaces of arbitrary sizes.

1. Convergence with perturbation order

Different quasi-degenerate spaces have been investigated, as summarized in Tab. I. For each of these spaces, we have studied the convergence of the energy levels with the perturbation order.

$2\nu_3$ quasi-degenerate space

The first quasi-degenerate space to investigate for calculating the energy levels of the $2\nu_3$-band, is of course the smallest one, that is to say, the 6-dimensional space corresponding to the $2\nu_3$-vibrational states. We do not report the results of low orders for this space, because although some levels were accurate, we feel that there were too many inversions for the results to be acceptable. We only report results for order 4, where only two inversions between a pair of close lying A_1 and E states occured, one for $J = 6$ and one for $J = 7$.

Fig. 1 displays the absolute errors with respect to the reference levels ($\nu_{ref} - \nu$) for different truncation thresholds on the spectator states. That is to say, instead of the infinite summation on the k_i appearing in Eq. (44), the k_i were limited to 530 (resp. 1232, 2143), which corresponds to the (vibrational) spectator states of the polyads $P0$ to $P5$ (resp. $P6$, $P7$). Note that for lower order corrections (order 2 and 3 namely) the summation was not infinite either but limited to all spectator eigenvectors within the calculated ones, that is to say $k_i \leq 16792$.

In Fig. 1, we see that each of the dots corresponding to the three different thresholds are superimposed. This means that, there is almost no difference in the calculated levels frequencies. This observation is confirmed by Tab. II, which compares the root mean square (RMS) of the relative error on level wave numbers for a given J-value. This remark is interesting, because the computational effort grows as the third power of the threshold for the fourth order correction. This is what is roughly confirmed in Tab. VII.

Another observation particularly evident on Tab. II, is the strong dependence on J-value of the quality of the results: more than a factor 2000 between $J = 1$ and $J = 7$. This hints to the slow convergence of the perturbation series for this choice of quasi-

degenerate space, since the lowest the J-value, the least the sensitivity to high order corrections. Moreover, a maximum absolute error of more than 3 cm^{-1} is observed on Fig. 1, which is fairly large for the computational effort.

$(\nu_1 + 2\nu_2, 2\nu_3)$ quasi-degenerate space

One obvious cause for the discrepancies of the $2\nu_3$-calculations, is the strong resonnance of this band with the closely lying $(\nu_1 + 2\nu_2)$-band constituted of an $A1$ and an E vibrational level. Extending the quasi-degenerate space to this band results in a 9-dimensional degenerate space, see Tab. I. This extension improves the perturbation series since at order 2, there is a single inversion observed between an $A2$ and an E state for $J = 7$. However, there is still some instabilities, since some order 3 values are worse than those of order 2, see Tab. III and Fig. 2, and the largest absolute error at these orders almost reach 4 cm^{-1} . The series is damped at order 4 (truncated at $P6$ on spectators), where absolute errors fall in the ± 1 cm^{-1} range. Tab. III shows that the RMS of relative errors for $J = 7$ levels, is also reduced by a factor 3. This is a significant improvement with respect to the $2\nu_3$-space but it costs roughly twice the computational effort for the construction of the effective Hamiltonian (see Tab. VII), which is the bottleneck of the calculation for large order and low dimensional quasi-degenerate spaces.

$(\nu_1 + \nu_3, 3\nu_2 + \nu_4, \nu_1 + 2\nu_2, 2\nu_3, 2\nu_2 + \nu_3, 4\nu_2)$ quasi-degenerate space

As an intermediate size quasi-degenerate space within the tetradecad, we gathered all the bands above the $2\nu_3$-band, and a roughly equivalent number of vibrational levels below the $2\nu_3$-band. The resulting space, denoted $(\nu_1+\nu_3)//\cdots//4\nu_2$ is 38-dimensional, see Tab. I. With this choice, the convergence of the series from order 2 to 4 (with spectators limited to $P5$ in the fourth order correction) is smooth, as shown by Fig. 3 and Tab. IV. Order 3 is already clearly better than order 4 of the $\nu_1+2\nu_2, 2\nu_3$-calculation, the maximum abolute error being less than 0.5 cm^{-1} , and the RMS of relative errors for $J = 7$ levels more than a factor 2 lower. Furthermore, this is achieved for a better computational cost, see Tab. VII.

Order 4 reduces further the maximum abolute error to slightly more than 0.3 cm^{-1} , and the ratio of RMS of relative errors for $J = 7$ over $J = 1$ is about 300, so almost an order of magnitude better than for the $2\nu_3$-calculation. This is essentially due to the improvement of high J-value levels.

P_4 quasi-degenerate space

The most natural quasi-degenerate space to select is arguably the one corresponding to the approximate quantum number $P = 4$, that is to say, the whole tetradecad itself. Though, the size of the space rises to 140, which prevents to perform order 4 calculations in reasonable time, and imposes to truncate the order 3 correction at $k_i \leq 4237$, that is to spectators within $P0 - P8$, in order to run the calculation in about 1.5 day on our cluster, see Tab. VII.

Fig. 4, shows that the maximum abolute error for order 2 is less than 0.03 cm^{-1} . This is about one order of magnitude lower than order 4 of the previous partitioning. Interestingly, if in the previous case, order 3 was almost systematically overshooting the energy eigenvalues, for $P4$ the reverse is observed. The RMS in Tab. V confirm that the $P4$-space gives much more accurate results than the previous quasi-degenerate spaces considered, while at order 2 the computational effort is still very light. This confirms the relevance of this intuitive choice of quasi-degenerate space.

$(P_0//\cdots//P_5)$, $(P_0//\cdots//P_6)$ and $(P_0//\cdots//P_7)$ quasi-degenerate spaces

Less intuitive but worth studying are larger spaces, which at order 1 should converge towards the exact eigenvalues. In order to partly balance the addition of $P5$, $P6$ and $P7$ to $P4$, it is reasonable to also add the lower states of $P0 - P3$, which give denominators with opposite signs in the perturbation series.

Order 1 of the $(P_0//\cdots//P_5)$-space gives correct levels with only one set of three levels (of symmetry F_2, E and A_1) permuted for $J = 7$. This was not the case of order 1 for the P_4-space, where many permutations were occuring. Even for $J = 1$ a permutation of an E and a F_1 level was observed. Let us recall that order 1 calculations are in fact variational. So, it is the variational principle that explains why all the absolute errors are negative, (we consider that the reference calculation variationnal space should essentially contain ours in spite of the projection on $F(7)$ and differences in modal basis functions). For $(P_0//\cdots//P_5)$, at order 1 the maximum abolute error is still as large as about 1 cm^{-1} , as seen on Fig. 5. However, it decreases with the inclusion of $P6$ and $P7$, as expected from the enlargement of the variational space, (see Figs. 6 and 7). Note that in all these variational calculations of increasing sizes, the Hylleraas-Undheim-MacDonald theorem[53,54] holds, so that every single level is improved as the space is enlarged. The RMS of Tab. VI give some quantitative ideas of the improvement with the size of the quasi-degenerate space. The latter can also be vizualized with the relative errors plotted in Fig. 8.

The situation is more complex when considering orders 2. Figs. 5, 6, and 7 (which is

at a larger scale) show that all order 2 calculations improve significantly order 1 results. However, the effect of the enlargement of the quasi-degenerate space is not systematic in contrast to order 1. Tab. VI shows that it depends on the J-value. The RMS for low J-values are better with the $(P_0//\cdots//P_5)$-space whereas for high J-values they are better with the $(P_0//\cdots//P_6)$-space. The quality of the results deteriorates with the $(P_0//\cdots//P_7)$-space for all J-values. The instability of order 2 results lies probably in the fact that the denominators in the perturbation series become very small with quasi-degenerate space enlargement, the gap with the upper polyads being smaller and smaller.

2. Convergence with quasi-degenerate space

It is also instructive to look at the relative errors as a function of the quasi-degenerate space for a fixed order of perturbation. This is what is proposed in Figs. 8 to 11. Order 1 has already been discussed in the previous section. At order 2 in Fig. 9, we see that the relative errors for the less accurate values vary by about three orders of magnitude with the wavelength. In contrast, for the $P4$ and larger spaces the variation is less pronounced. For the $(P_0//\cdots//P_6)$-space, it is rather flat with all relative errors falling below 10^{-6}. Fig. 10 which displays order 3 relative errors shows a clear general improvement of the results and a milder wavelength dependency of the worst levels with the widening of the quasi-degenerate space. On Fig. 11, we also see a clear general improvement with increasing sizes of the quasi-degenerate spaces, (the spectator truncation thresholds are reduced with the increase of space dimension, but on the basis of Fig. 1 and Tab. II, one does not expect that this affects the results significantly). However, the wavelength dependency of the worst levels is strong for all calculations. This suggests a slow series convergence for quasi-degenerate spaces smaller than the tetradecad. This is not surprising because small denominators will occur due to small energy differences between the states in the quasi-degenerate space and the other states of the tetradecad excluded from this space. So, a quasi-degenerate space larger than or equal to $P4$ seems necessary to obtain a well-behaved perturbation series, at least up to order 3. But it must be strictly smaller than the $(P_0//\cdots//P_7)$-space to prevent the occurence of small denominators resulting from the tiny $P_7//P_8$-gap, as was invoked in the previous section to explain order 2 results.

3. Computational cost

Putting all previous observations together, we see that, in order to reach a relative accuracy better than say 2.10^{-6} on $(J = 7)$-levels, one needs an order 3 calculation for the $P4$-space, or an order 2 calculation for $(P_0//\cdots//P_k)$-spaces with $k = 5, 6$ or 7, or of course an order 1 i.e. a variational calculation for an even larger quasi-degenerate space. One needs to look at the computational cost of these calculations to select the most efficient one for a given accuracy goal.

Tab. VII gives orders of magnitude of cpu times required for the construction of the effective super-Hamiltonians. For a given perturbation order, they scale linearly with the number of symmetry-unique blocks of the super-Hamiltonians, that is to say as $\frac{N_{\mathbf{x}}(N_{\mathbf{x}}+1)}{2}$, for a quasi-degenerate space of dimension $N_{\mathbf{x}}$. The scaling with perturbation order depends drastically on the truncation threshold since the corrective terms of order n require $(n-1)$ nested loops on spectators states. As already stated, for small quasi-degenerate spaces, the construction of the super-Hamiltonian is the bottleneck of the calculation. However, for large ones, the cost of the diagonalization of the super-Hamiltonian matrix, which is of size $N_{\mathbf{x}} \times (2J+1)$ for J-levels must be taken into account and will eventually dominate as $N_{\mathbf{x}}$ and J increase. This is also, of course, the dominant cost for order 1 calculations. We have not reported diagonalization cost as they depend on the algorithm, library, plateform and so on, employed but generally speaking one expects a scaling as the matrix size to the third power. So, a factor 12.6 will incur when going from $(P_0//\cdots//P_5)$ to $(P_0//\cdots//P_6)$-space and another factor 5.3 from $(P_0//\cdots//P_6)$ to $(P_0//\cdots//P_7)$-space.

In supplementary material, we have reported our most accurate perturbational results, corresponding to order 2 of perturbation and the $(P_0//\cdots//P_6)$-space. For $J = 7$, the effective super-Hamiltonian matrix to diagonalize was of size 18480. This is to be compared with the size of the reference variational calculation, that is to say, with the rovibrational direct product basis set size of 171870 for the same J-value. (In both cases we do not take into account symmetry, which in methane can reduce sizes by a factor ten). Clearly, it is worth spending the 2.1 hours of CPU time required to build the order 2 effective super-Hamiltonian. Note that the computation of order 2 corrective terms is not parallelized in our code, in contrast with higher order corrections.

III. CONCLUSION

This article has introduced a generalization of our previous effective Hamiltonian method[55] to the case of quasi-degenerate zero order eigenspaces. Our formalism encompasses both the Rayleigh-Ritz variational method based on the diagonalization of an Hamiltonian matrix (order 1 of quasi-degenerate perturbation theory with all zero order states considered formally as quasi-degenerate even if in practice their associated energies differ by several orders of magnitude) and the Rayleigh-Schrödinger generalized perturbation method (when a single zero order state, possibly exactly degenerate, is included in the quasi-degenerate space). Between these extreme cases, the new formalism allows one to tune up the calculation by playing on only a few simple parameters such as the perturbation order, the size of the quasi-degenerate space, the spectator state truncation thresholds for corrective terms of order 2 and higher, so as to solve the eigenvalue problem in the most economical way for a given accuracy goal.

Our application to methane shows that:
(i) A similar accuracy can be reached for the tetradecad than that obtained for the ground state in previous applications[4,42,56].
(ii) The computational effort can be reduced by introducing perturbative corrections with respect to large variational calculations without sacrifying significantly the accuracy.

Further developments could include mould calculus techniques to improved our non-commuting effective operator series speed of convergence, such series being precisely what is called a "mould" in mathematics. Also, as suggested by other authors[1], *ab initio* effective super-Hamiltonian can be useful to solve the inverse problem raised by spectroscopic data processing. In fact, it is well-known in mathematics that inverse problems are ill-defined and that there are three possible reasons for that[57,58]:
1) the solution may not exist,
2) it may not be unique,
3) it may be unstable with respect to small changes in the data,
the later being the most difficult to fix. The most common regularization of inverse problem unstability is known as Tikhonov regularization[59]. It consists in solving a stabilized inverse problem whose solution is the solution of the initial inverse problem that is the closest of a reasonable guess solution. This is precisely what can be achieved by using our ab initio effective super-hamiltonians as a guess, in the field of molecular spectroscopy.

IV. ACKNOWLEDGEMENTS

This work was supported by the GENCI grant N° x2012086823 and the grant CARMA ANR-12-BS01-0017. The authors acknowledge the SIGAMM Mesocentre for hosting the CONVIV code project, as well as for providing computer facilities. This work was granted access to the HPC and vizualization resources of the "Centre de Calcul Interactif" hosted by University Nice Sophia Antipolis.

REFERENCES

[1]Vl. G. Tyuterev, Sergei Tashkun, Michael Rey, Roman Kochanov, Andrei V. Nikitin, and Thibault Delahaye J. Phys. C: Solid State Phys. **A117**, 13779 (2013).

[2]P. Cassam-Chenaï and J. Liévin, Int. J. Quantum Chem. **93**, 245-264 (2003).

[3]P. Cassam-Chenaï, J. Quant. Spectrosc. Radiat. Transfer **82**, 251-277 (2003).

[4]P. Cassam-Chenaï, Y. Bouret, M. Rey, S. A. Tashkun, A. V. Nikitin and Vl. G. Tyuterev, Int. J. Quantum Chem. , in press (2011).

[5]Nixon, C. A. , Temelso, B., Vinatier S., et al., 2012, Astrophys. J. **,**, 7 (4).9, 159

[6]Legget, S. K., Marley, M. S., Freedmann, R., et al., 2007, Astrophys. J. **,** 6 (6).7, 537

[7]Swain, M. S. Vasisht, G., & Tinetti, G., 2008, Nature, 452, 329

[8]Swain, M. S. Vasisht, G., Tinetti, G., et al., 2009, Astrophys. J. **,** 6 (9).0, L114

[9]Swain, M. R., Deroo, P., Griffith, C. A., Tinetti, G., et al., 2010, Nature, 463, 637

[10]Tinetti, G., Liang, M.-C., Vidal Madjar, A., Ehrenreich, D., Lecavelier des Etangs, A, & Yung, Y., 2007b, Astrophys. J. **,** 6 (5).4, L99

[11]Hirtzig, M., Bézard, B., Lellouch, E. et al, 2013, Icarus, 226, 470

[12]Moses, J. I., Visscher, C., Fortney, J. J., et al., 2011, Astrophys. J. **,** 7 (3).7, 15

[13]de Bergh, C., Courtin, R., Bézard, B. et al, 2012, Planet. Space Sci., 68, 85

[14]Champion, J.-P., 1977, Can. J. Phys., 55, 1802

[15]Boudon, V., Champion, J.-P., Gabard, T. et al., 2004, J. Mol. Spectrosc., 228, 620

[16]Nikitin, A. V., Rey, M., Champion, J.-P., & Tyuterev, Vl. G., 2012, J. Quant. Spectrosc. Radiat. Transfer, 113, 1034

[17]Brown, L. R., Sung, K., Benner, D. C. et al., 2013, J. Quant. Spectrosc. Radiat. Transfer, 130, 201

[18]Nikitin, A. V. , Boudon, V. Wenger. Ch., et al., 2013a, Phys. Chem. Chem. Phys., 15, 10071

[19]Campargue, A. Leshchishina, O., Wang, L. et al., 2013, J. Mol. Spectrosc., 291, 16

[20]D. W. Schwenke and H. Partridge, Spectr. Acta **A 57**, 887 (2001).

[21]D. W. Schwenke, Spectr. Acta **A 58**, 849-861 (2002).

[22]R. Marquardt, M. Quack, J. Phys. Chem. **108**, 3166 (2004).

[23]C. Oyanagi, K. Yagi, T. Taketsugu, K. Hirao, J. Chem. Phys **124**, 064311 (2006).

[24]J. Wu, X Huang, S. Carter and J. M. Bowman, Chem. Phys. Lett. **426**, 285 (2006).

[25]M. Rey, A. V. Nikitin and Vl. G. Tyuterev, Phys. Chem. Chem. Phys. **15**, 10049 (2013).

[26]C. Fábri, T.Furtenbacher, A. G. Császár, Mol. Phys. **112**, 2462 (2014).

[27]S. N. Yurchenko, J. Tennyson, "ExoMol line lists IV: The rotation-vibration spectrum of methane up to 1500 K", Monthly Notices of the Royal Astronomical Society 440, 1649-1661 (2014).

[28]X. G. Wang et T. Carrington, J. Chem. Phys **141**, 154106 (2004).

[29]S. L. Mielke, D. G. Truhlar, J. Chem. Phys **142**, 044105 (2015).

[30]P. H. Flamant, G. Ehret, P. Bousquet, J. Marshall, B. Millet, M. Alpers, C. Pierangelo, C. Stephan, *MERLIN: a new Franco-German 'MEthane Remote sensing LIdar missioN*, in Proceedings of the IWGGMS-10 (10th International Workshop on Greenhouse Gas Measurements from Space, ESA/ESTEC, The Netherlands, May 5-7, 2014).

[31]D.Klein, J. Chem. Phys **61**, 786 (1974).

[32]Yu. S. Makushkin, Vl. G. Tyuterev, *Perturbation Methods and Effective Hamiltonians in Molecular Spectroscopy*, Nauka, Novosibirsk, (1984) *[in Russian].*

[33]J. K. G. Watson, Mol. Phys. **103**, 3283 (2005).

[34]J. des Cloizeaux, nucl. phys. **20**, 321 (1960).

[35]C. Soliverez, J. Phys. C: Solid State Phys. **2**, 2161 (1969).

[36]J. H. Van Vleck, Phys. Rev. **33**, 467 (1929).

[37]E. C. Kemble, "Fundamentals of Quantum Mechanics" (Dover, New York, 1937), p. 395

[38]H. Primas, Rev. Mod. Phys. **35**, 710 (1963).

[39]L. N. Buleavski, Zh. Eksp. Teor. Fiz. **51**, 230 (1966). [English translation in Sov. Phys. -JETP **24**, P. 154 (1967)].

[40]J. K. G. Watson, Mol. Phys. **15**, 479-490 (1968).

[41]V. Boudon, M. Rey, M. Loëte, J. Quant. Spectrosc. Radiat. Transfer **98**, 394 (2006).

[42]P. Cassam-Chenaï and J. Liévin, J. Chem. Phys **136**, 174309 (2012).

[43]G. Rousseau, *Rapport de stage L3-Magistre 1 de Physique Fondamentale*, (Universit Paris-sud 11, 2013)

[44]R. Winkler, *Spin-Orbit Coupling Effects in Two-Dimensional Electron and Hole Systems*, Springer Tracts in Modern Physics **191**, (Springer, Berlin, Heidelberg, 2003).

[45]A. V. Nikitin, M. Rey and Vl. G. Tyuterev, Chem. Phys. Lett. **501**, 179 (2011).

[46]M. Rey, A. V. Nikitin, and Vl. G. Tyuterev, J. Chem. Phys **136**, 244106 (2012).

[47]A. Kratzer, Z. Physik 3,(1920) 289

[48]Don Secrest, J. Chem. Phys **89**, 1017 (1988).

[49]P. Cassam-Chenaï, J. Liévin, Journal of Computational Chemistry **27**, 627-640 (2006).

[50]P. Cassam-Chenaï, A. Ilmane, J. Math. Chem. **50**, 652-667 (2012).

[51]M. Rey, V. Boudon, Ch. Wenger, G. Pierre, B. Sartakov, J. Mol. Spectrosc. **219**, 313 (2003).

[52]M. Rey, A. V. Nikitin and Vl. G. Tyuterev, J. Chem. Phys **141**, 044316 (2014).

[53]E. A. Hylleraas and B. Undheim, Z. Phys. 65 759 1930

[54]J. K. L. MacDonald, Phys. Rev. 43 830 1933

[55]P. Cassam-Chenaï, J. Math. Chem. **49**, 821 (2011).

[56]P. Cassam-Chenaï and J. Liévin, J. Mol. Spectrosc. **291**, 77-84 (2013). And supplementary material.

[57]J. Hadamard, "La théorie des équations aux dérivées partielles", (Ed. Scientifiques, Peking, 1964).

[58]D. Courant and D. Hilbert, *Methods of Mathematical Physics, Vol. 2*, Interscience publishers, New York (1962)

[59]A. Tikhonov, V. Arsenine, "Méthodes de résolution de problèmes mal posés", (Ed. Mir, Moscou, 1974).

TABLES AND FIGURES CAPTION

Label	vib. states	wave numbers (cm^{-1})	size
$2\nu_3$	(201 - 206)	5968.27821 – 6043.82444	6
$(\nu_1 + 2\nu_2)//2\nu_3$	(198 - 206)	5939.16404 – 6043.82444	9
$(\nu_1 + \nu_3)//\cdots//4\nu_2$	(183 - 220)	5861.06072 – 6124.50383	38
P4	(81 - 220)	5123.64379 – 6124.50383	140
P0-P5	(1 - 530)	0.00000 – 7588.09422	530
P0-P6	(1 - 1232)	0.00000 – 9190.45568	1232
P0-P7	(1 - 2143)	0.00000 – 10454.77160	2143
P0-P8	(1 - 4237)	0.00000 – 12157.21552	4237

TABLE I. Quasi-degenerate vibrational spaces. The labels of the groups are those used throughout the article. The " vib. states" column indicates the numbers of the vibrational levels considered as "quasi degenerate". The numerotation starts from 1 and counts all exactly degenerate vectors independently. The corresponding wave numbers are those obtained by our $J = 0$ variational calculation. The size of the group correspond to $N_{\mathbf{x}}$: the square root of the number of blocks of the super-Hamiltonian.

J	o4-530	o4-1232	o4-2143
1	8.79774e-08	8.80757e-08	8.74808e-08
2	4.09010e-07	4.09076e-07	4.22824e-07
3	1.11117e-06	1.04565e-06	1.01125e-06
4	5.12308e-06	4.89975e-06	4.79271e-06
5	3.73108e-05	3.73375e-05	3.77563e-05
6	9.73328e-05	9.75357e-05	9.84951e-05
7	1.70857e-04	1.71405e-04	1.72811e-04

TABLE II. Convergence of relative errors for the $2\nu_3$ quasi-degenerate space fourth order perturbation with the spectator sum truncation threshold of the order 4 corrective term. "o4-530" (resp. "o4-1232", "o4-2143") means that the infinite summation on the k_i's appearing in Eq. (44), was limited to $k_i \leq 530$ (resp. 1232, 2143). See main text for details.

J	o2	o3	o4-1232
1	4.69346e-07	2.09936e-07	8.90504e-08
2	2.05879e-06	1.80785e-06	2.67716e-07
3	8.07932e-06	4.18744e-06	1.02595e-06
4	2.33342e-05	1.04137e-05	4.77393e-06
5	5.34091e-05	6.70347e-05	1.77674e-05
6	1.21060e-04	1.76789e-04	4.69836e-05
7	1.92754e-04	2.91982e-04	5.91106e-05

TABLE III. Convergence of relative errors for the $(\nu_1 + 2\nu_2)//2\nu_3$ quasi-degenerate space and different perturbation orders. "o2" means order 2, "o3": order 3, "o4-1232": order 4 with truncation as in Tab. (II).

J	o2	o3	o4-530
1	3.31135e-07	9.08082e-08	8.21053e-08
2	1.01615e-06	3.47092e-07	1.24435e-07
3	2.52242e-06	1.35844e-06	2.80655e-07
4	5.80215e-06	3.81181e-06	1.06746e-06
5	1.41850e-05	9.45332e-06	3.53232e-06
6	2.95286e-05	1.94261e-05	1.00181e-05
7	6.17759e-05	3.28615e-05	2.67881e-05

TABLE IV. Convergence of relative errors for the $(\nu_1+\nu_3)//\cdots//4\nu_2 \equiv (\nu_1+\nu_3, 3\nu_2+\nu_4, \nu_1+2\nu_2, 2\nu_3, 2\nu_2+\nu_3, 4\nu_2)$ quasi-degenerate space and different perturbation orders. "o2": order 2, "o3": order 3, "o4-530": order 4 with truncation as in Tab. (II).

J	o2	o3-4237
1	7.46591e-08	8.94996e-08
2	1.92208e-07	1.47123e-07
3	4.23416e-07	2.36744e-07
4	6.87447e-07	3.54659e-07
5	1.16016e-06	6.69531e-07
6	1.84134e-06	1.11404e-06
7	2.88847e-06	1.72081e-06

TABLE V. Convergence of relative errors for (P_4) quasi-degenerate space and different perturbation orders. "o2": order 2, "o3-4237": order 3 with infinite summation on the k_i's appearing in Eq. (41) limited to $k_i \leq 4237$.

	o1			o2		
J	$(P_0//\cdots//P_5)$	$(P_0//\cdots//P_6)$	$(P_0//\cdots//P_7)$	$(P_0//\cdots//P_5)$	$(P_0//\cdots//P_6)$	$(P_0//\cdots//P_7)$
1	3.74223e-06	3.49298e-06	6.68670e-07	8.08064e-08	8.73907e-08	9.11457e-08
2	1.13858e-05	1.04411e-05	2.15160e-06	1.13273e-07	1.36636e-07	1.50637e-07
3	2.32933e-05	2.06020e-05	4.24520e-06	1.56365e-07	2.12608e-07	2.63614e-07
4	4.05039e-05	3.44394e-05	7.25150e-06	1.92121e-07	2.99005e-07	4.57559e-07
5	6.40288e-05	5.08010e-05	1.01577e-05	4.44408e-07	4.33823e-07	8.03109e-07
6	9.46963e-05	7.00951e-05	1.39972e-05	8.83586e-07	5.31268e-07	1.24737e-06
7	1.34007e-04	9.23214e-05	1.82919e-05	1.67086e-06	6.51010e-07	1.93673e-06

TABLE VI. Convergence of relative errors for $(P_0//\cdots//P_5)$, $(P_0//\cdots//P_6)$ and $(P_0//\cdots//P_7)$ quasi-degenerate spaces and different perturbation orders. "o1": order 1, "o2": order 2.

quasi-deg. space	nb. blocks	o2	o3-4237	o3	o4-530	o4-1232	o4-2143
$2\nu_3$	21	0.2 s	-	1.0 h	3.4 h	2.1 d	11 d
$(\nu_1+2\nu_2)//2\nu_3$	45	0.5 s	-	2.1 h	7.3 h	4.6 d	*23.7 d*
$(\nu_1+\nu_3)//\cdots//4\nu_2$	741	7.4 s	-	35.5h	5.0d	*75.6 d*	-
P4	9870	2 min	30.8 h	*19.7 d*	*66.6 d*	-	-
P0-P5	140715	24 min	*18.3 d*	*281.0 d*	-	-	-
P0-P6	759528	2.1 h	*98.9 d*	-	-	-	-
P0-P7	2297296	6.4 h	-	-	-	-	-

TABLE VII. Orders of magnitude of CPU times required to construct superHamiltonians on a node of an HP cluster (each node has 2 processors Intel(R) E5-2670 - 2.60 GHz - 8 cores with 64 GigaBytes memory). The column "nb. blocks" shows the number of symmetry unique blocks to be calculated, that is to say, $\frac{N_{\mathbf{x}}(N_{\mathbf{x}}+1)}{2}$, for a quasi-degenerate space of dimension $N_{\mathbf{x}}$. The notation "on-X" refers to order n correction with sum on spectator basis functions truncated at the X^{th} function. If no "X" is specified all the 16792 vibrational functions were used. Only orders 3 and 4 superHamiltonian corrections were parallelized with openmp, order 2 was not. All calculations were run with 16 threads. Numbers in italics were extrapolated as calculations were not actually run.

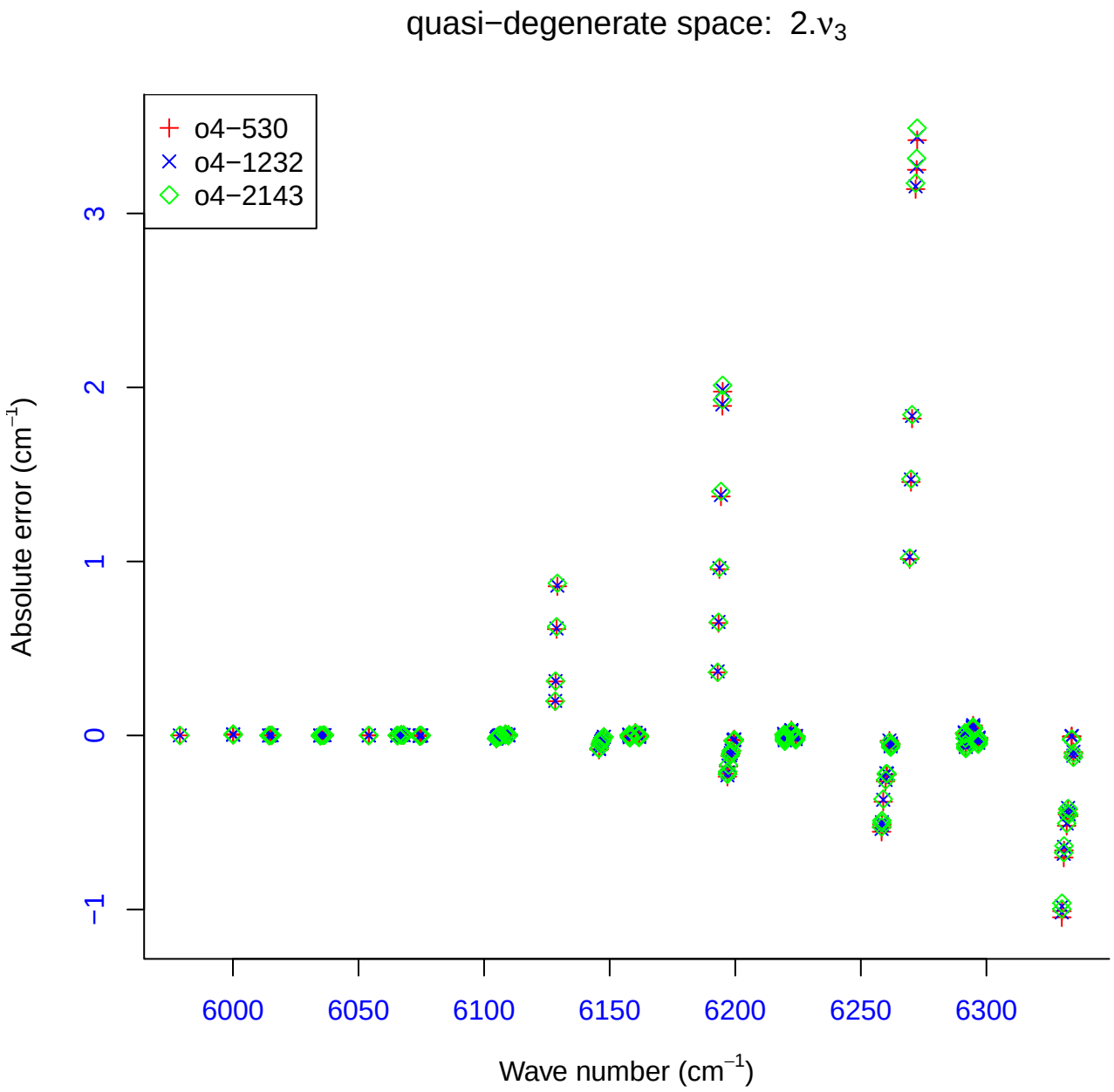

FIG. 1. Convergence of order 4 perturbation series with truncation threshold: 530 red plus signs, 1232 blue times signs, 2143 green diamonds.

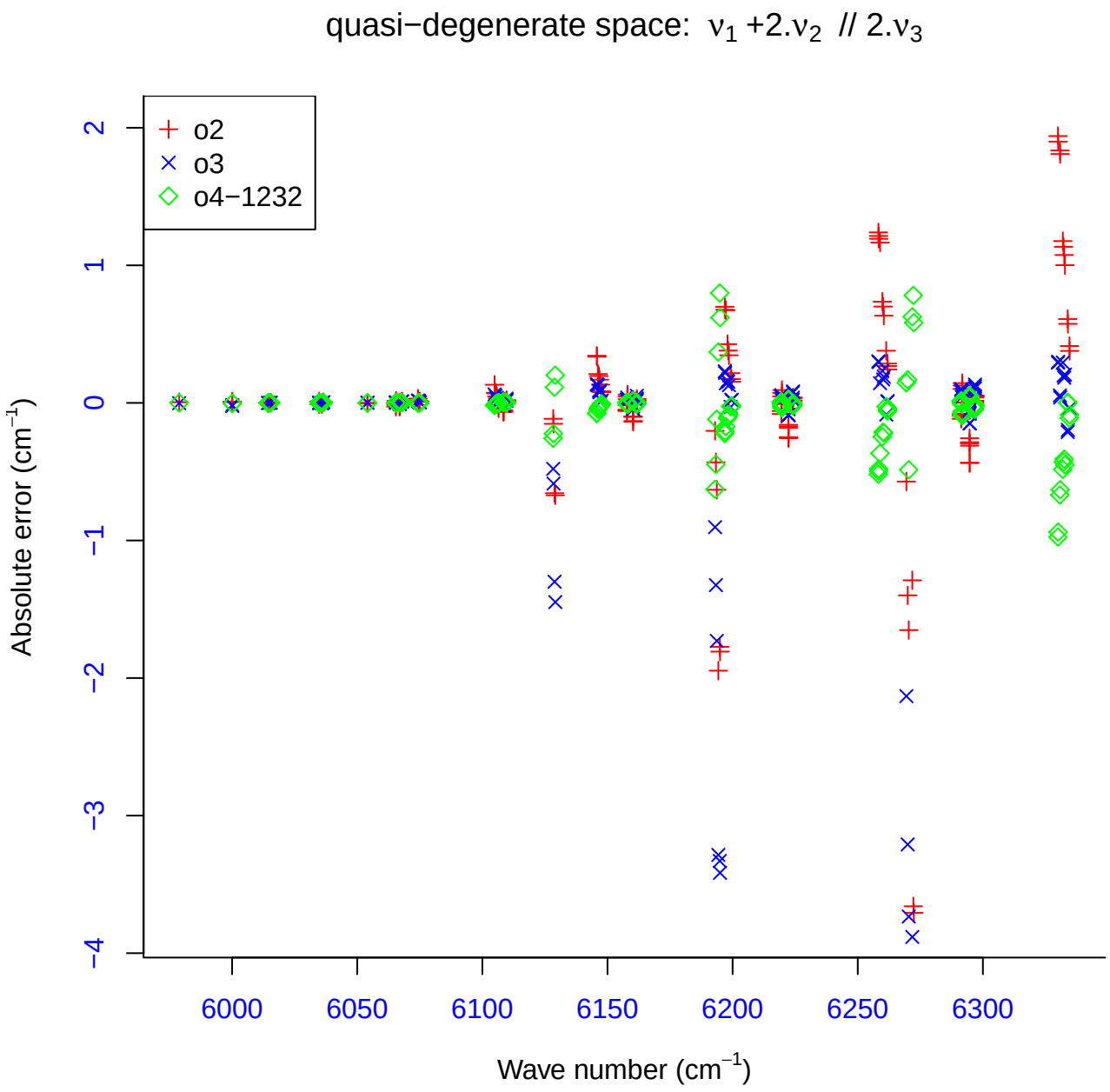

FIG. 2. Convergence of perturbation series for $(\nu_1 + 2\nu_2, 2\nu_3)$ quasi-degenerate space. See Tab. III for definition of acronyms.

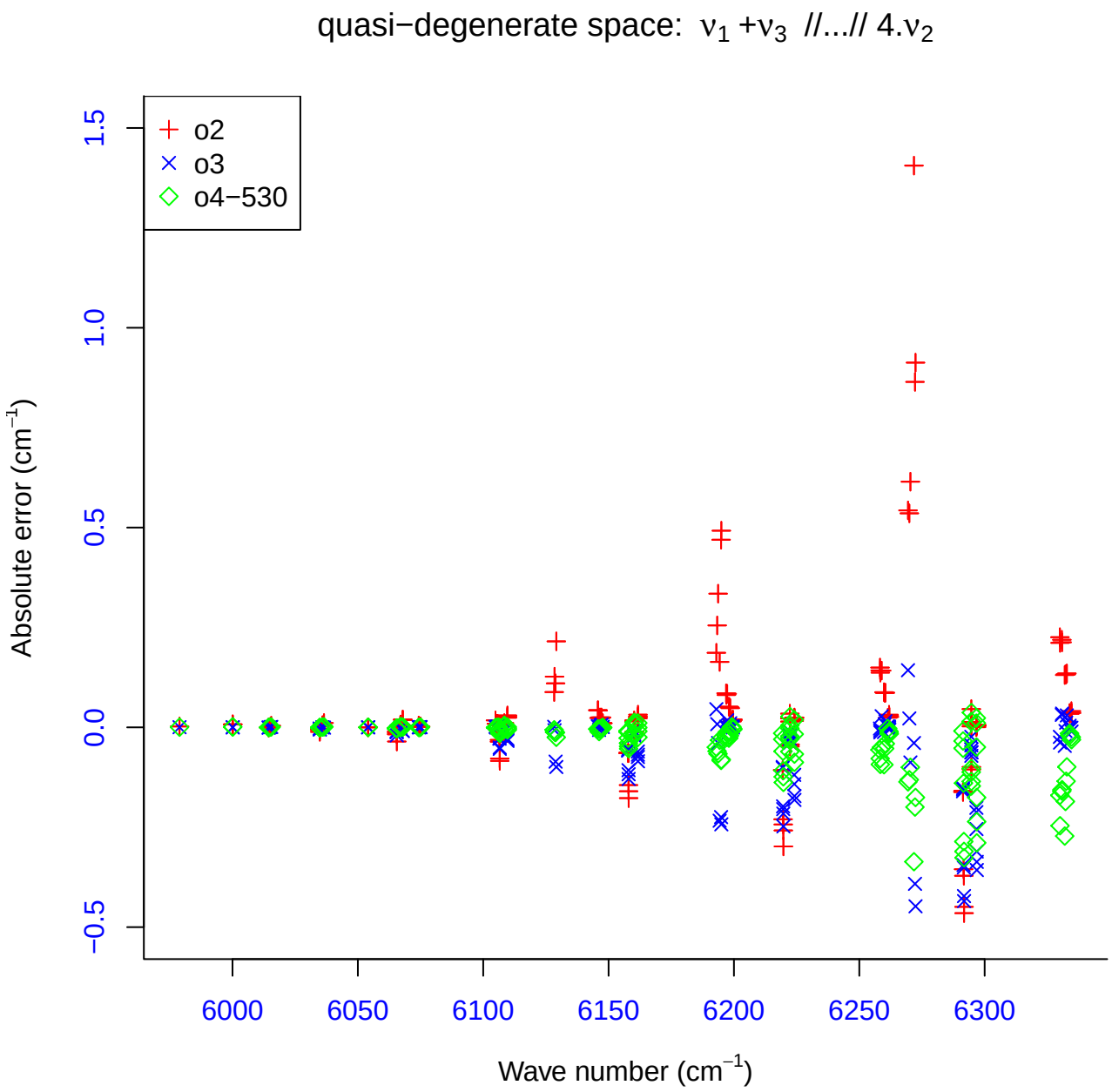

FIG. 3. Convergence of perturbation series for $(\nu_1+\nu_3, 3\nu_2+\nu_4, \nu_1+2\nu_2, 2\nu_3, 2\nu_2+\nu_3, 4\nu_2)$ quasi-degenerate space. See Tab. IV for definition of acronyms.

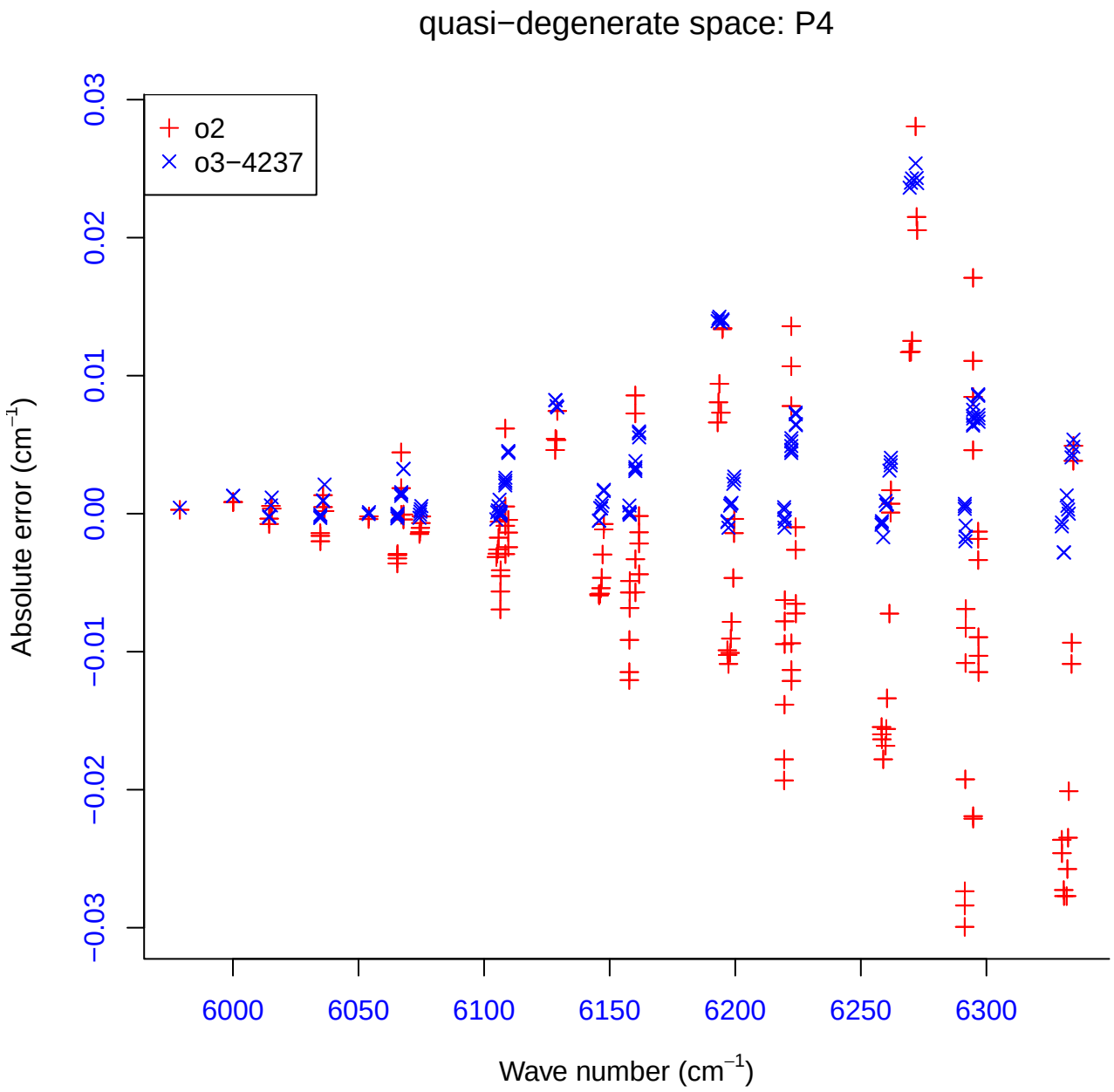

FIG. 4. Convergence of perturbation series for (P_4) quasi-degenerate space. See Tab. V for definition of acronyms.

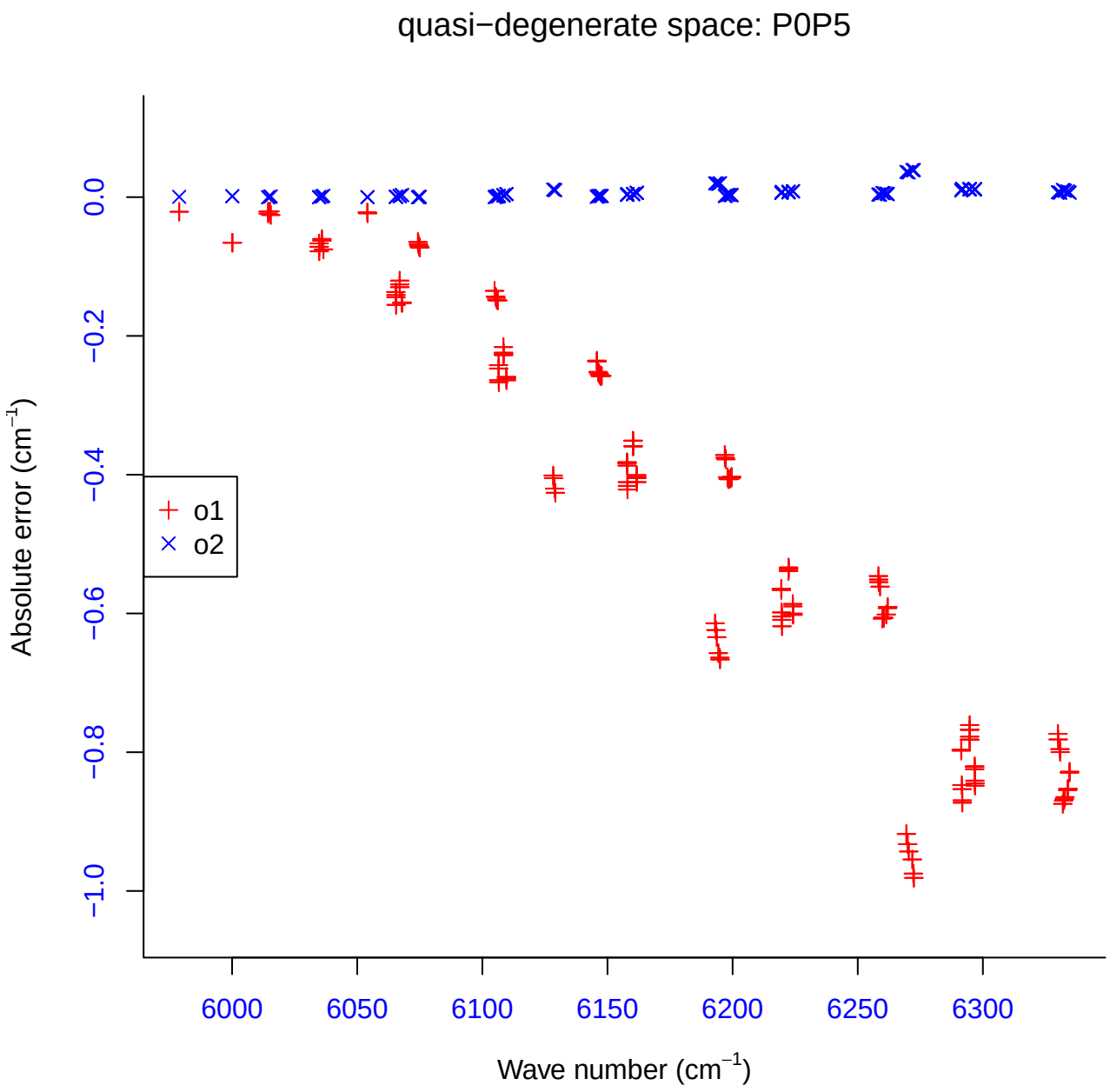

FIG. 5. Convergence of perturbation series for $(P_0//\cdots//P_5)$ quasi-degenerate space. See Tab. VI for definition of acronyms.

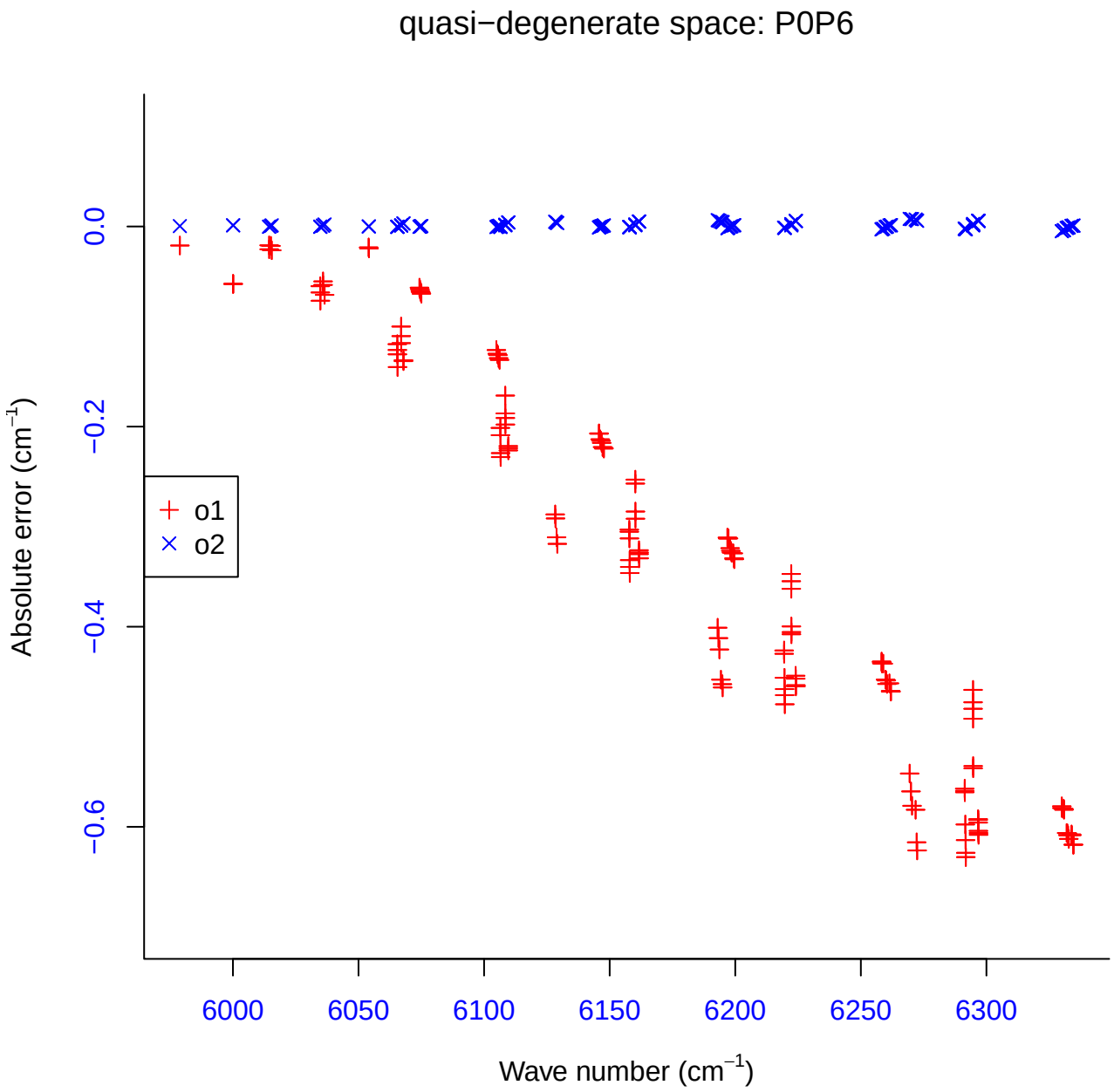

FIG. 6. Convergence of perturbation series for $(P_0//\cdots//P_6)$ quasi-degenerate space. See Tab. VI for definition of acronyms.

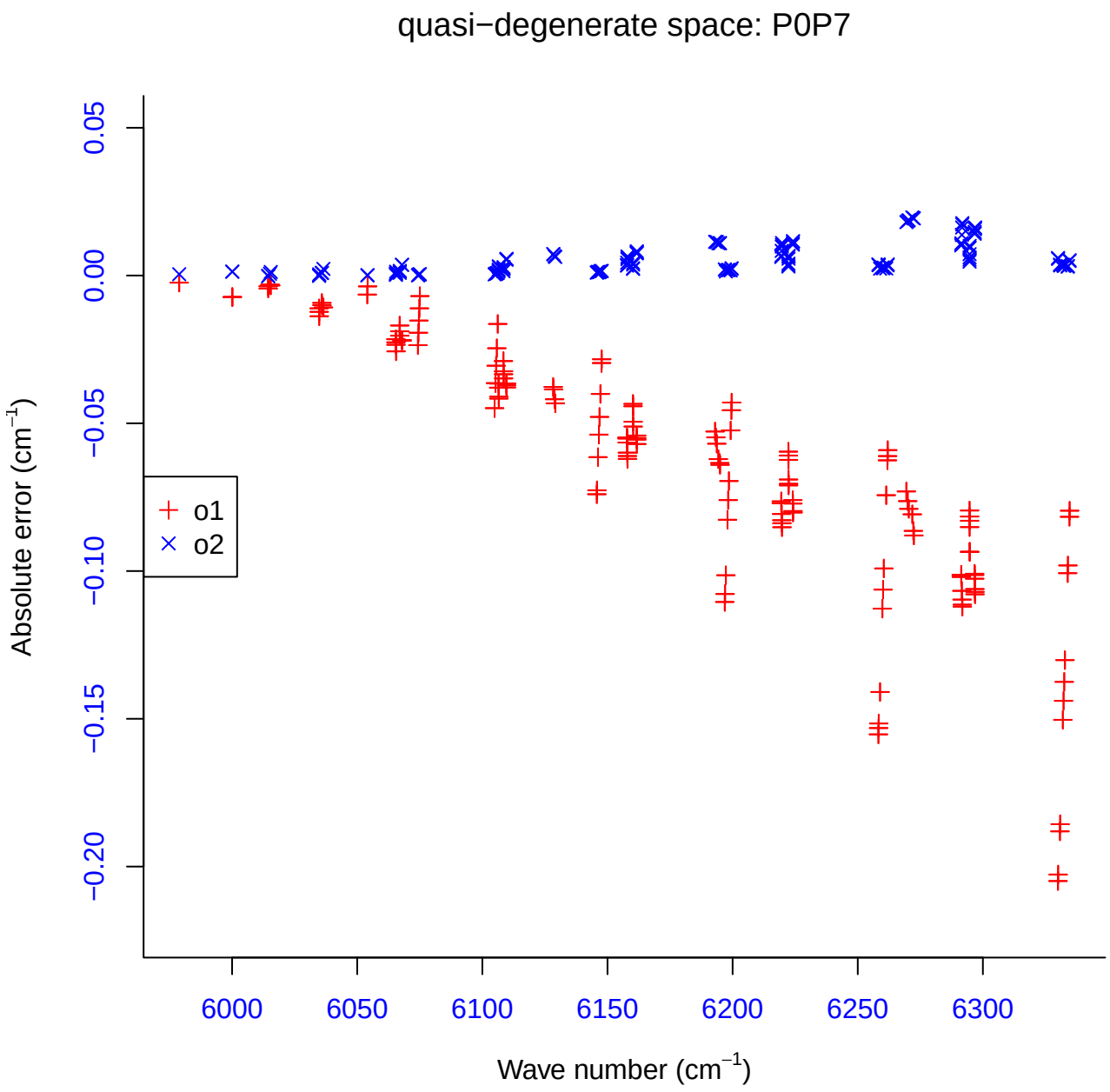

FIG. 7. Convergence of perturbation series for $(P_0//\cdots//P_7)$ quasi-degenerate space. See Tab. VI for definition of acronyms.

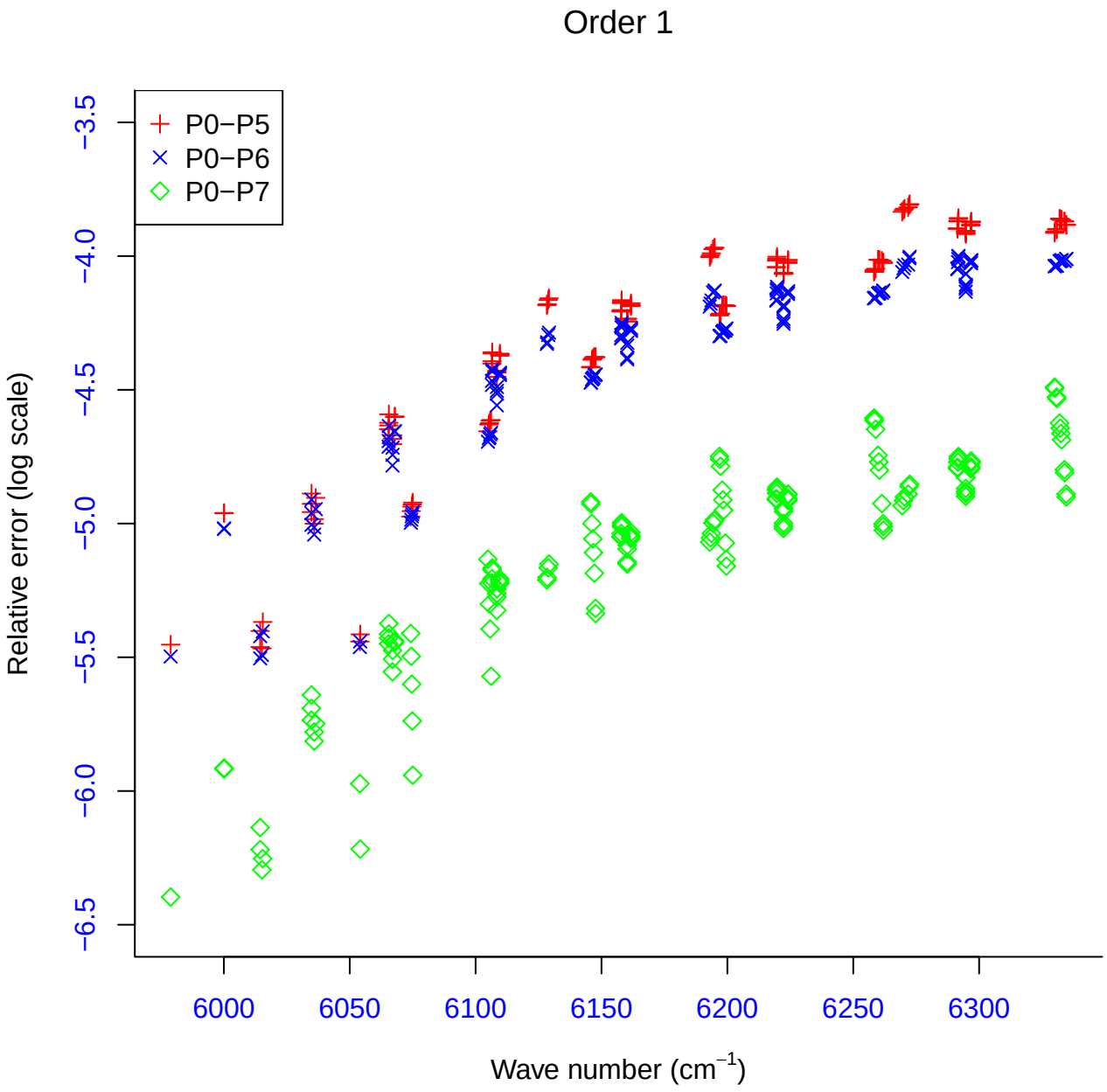

FIG. 8. Convergence of order 1 perturbation series with quasi-degenerate space.

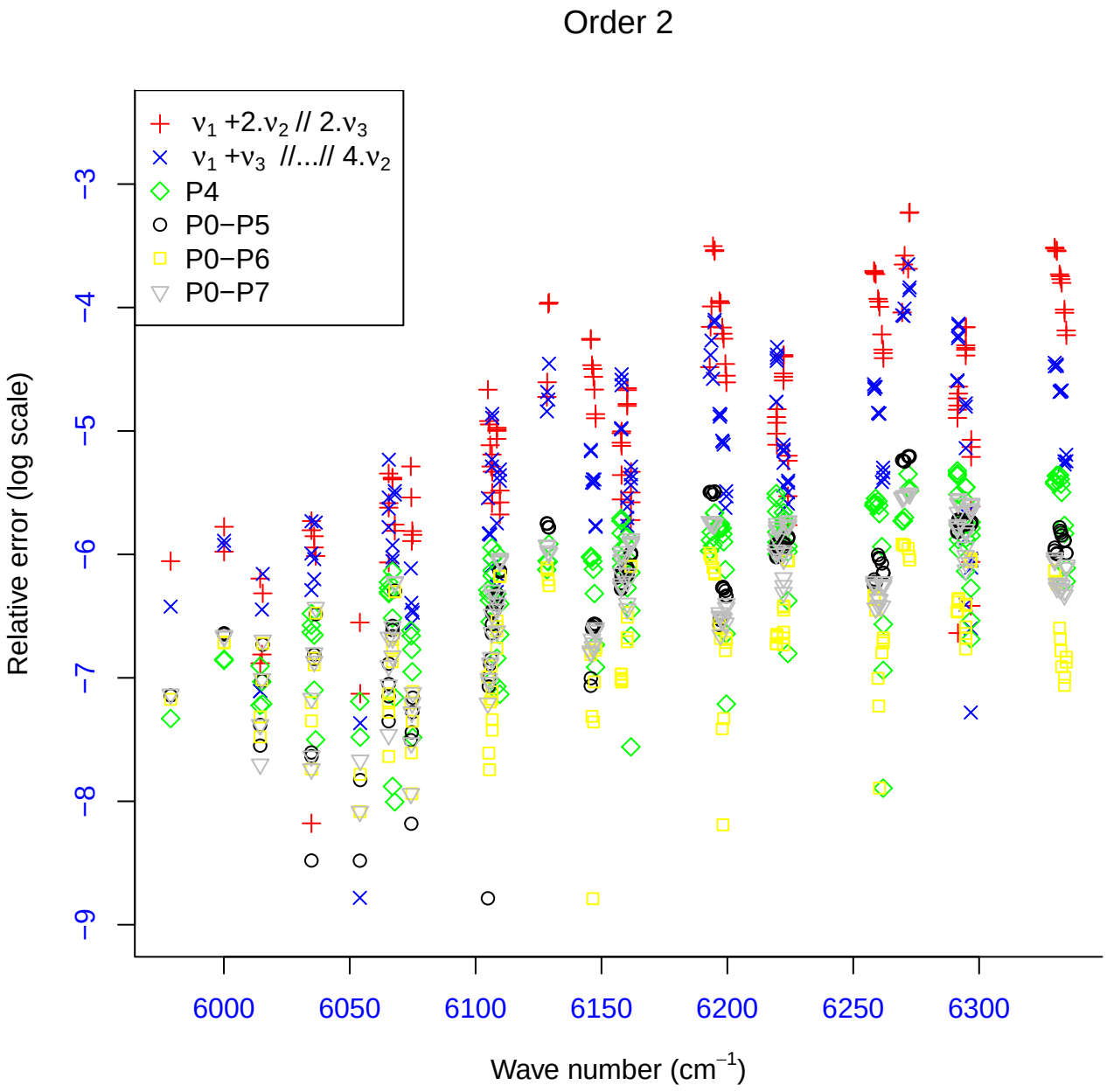

FIG. 9. Convergence of order 2 perturbation series with quasi-degenerate space.

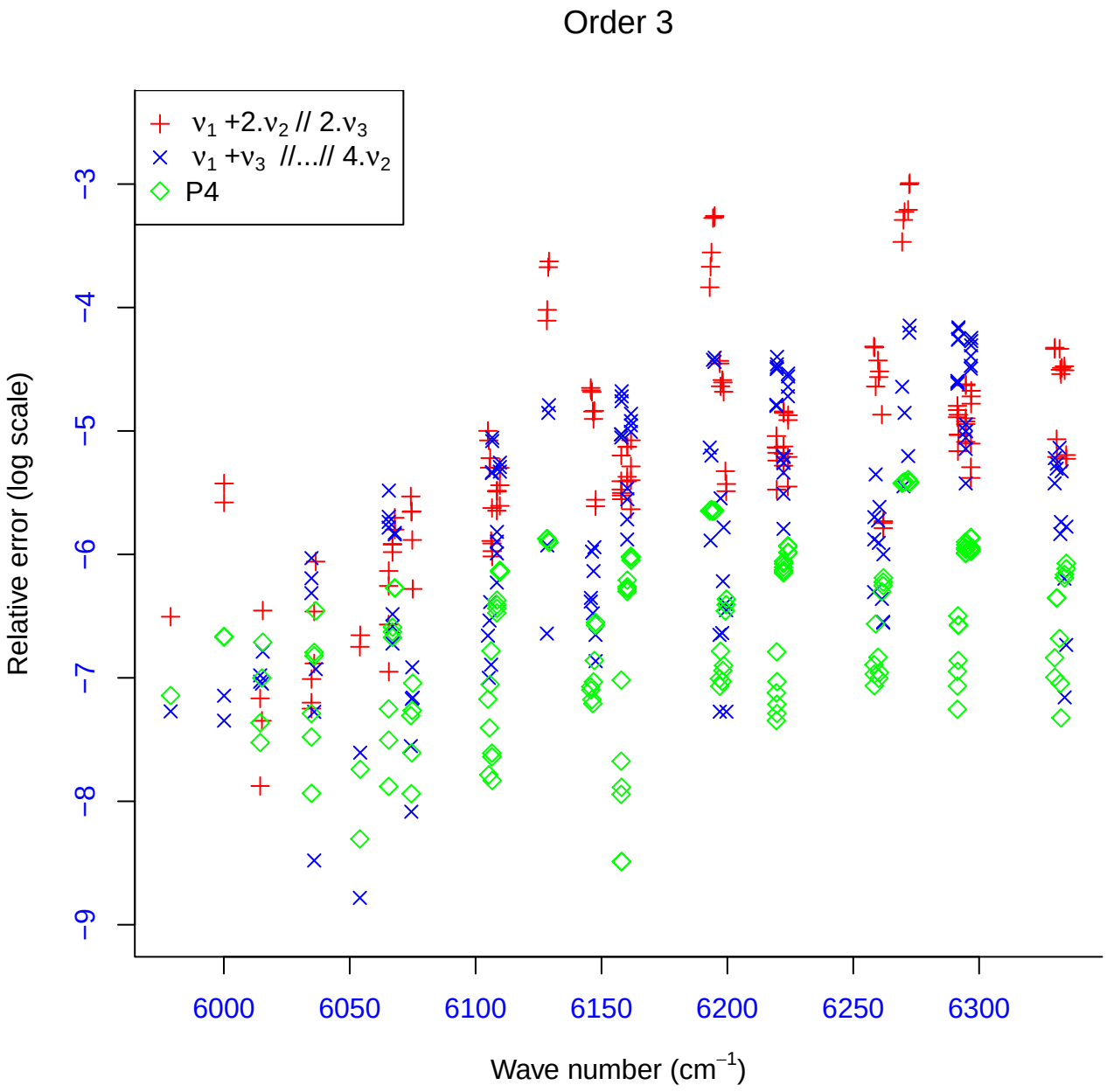

FIG. 10. Convergence of order 3 perturbation series with quasi-degenerate space.

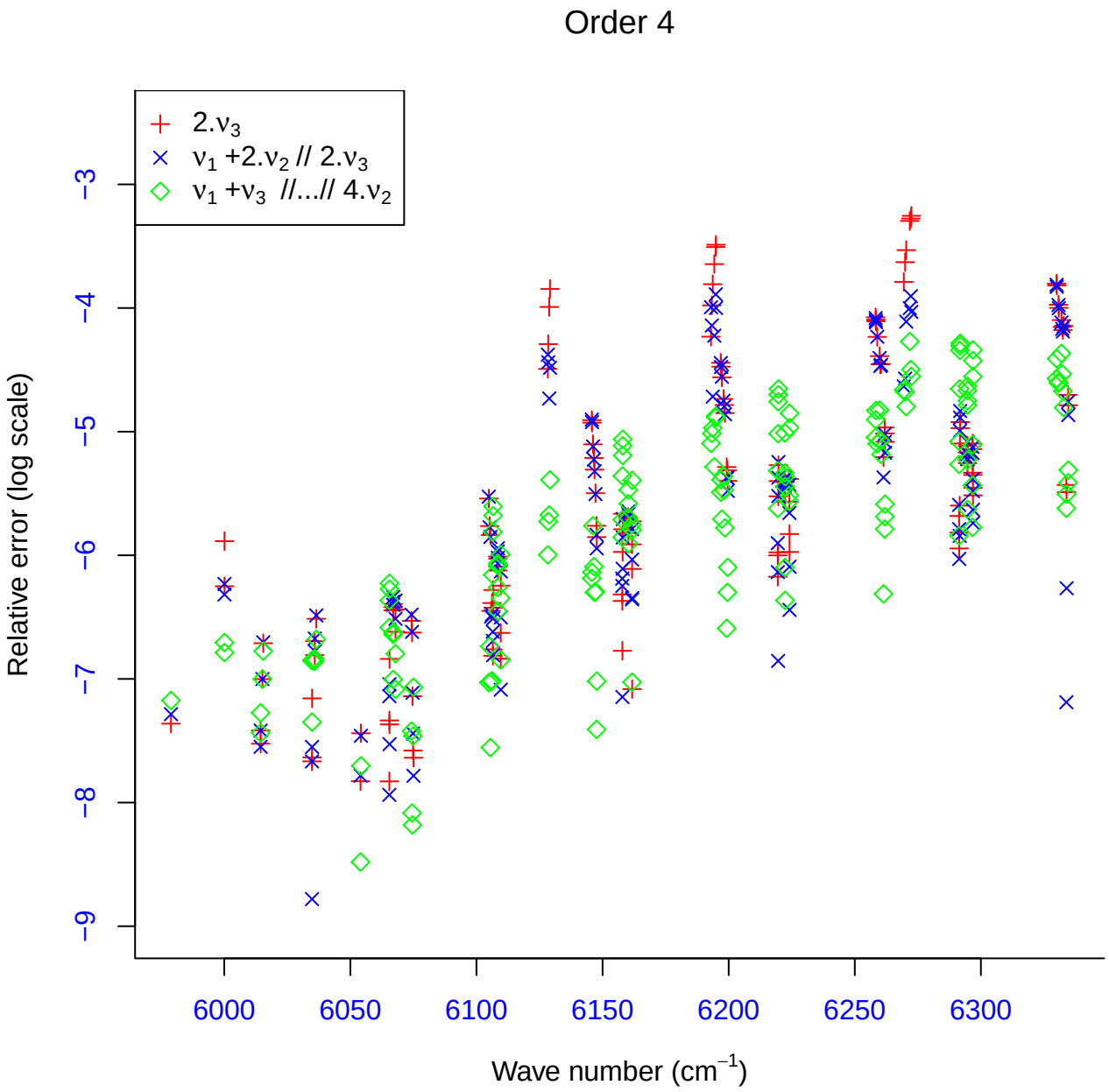

FIG. 11. Convergence of order 4 perturbation series with quasi-degenerate space.

Approximate and reference band centers (in cm^{-1})

VMFCI (27535 cm^{-1})	Ref. (F13P7)	difference
1310.744	1310.742	0.002
1533.315	1533.314	0.001
2587.285	2587.267	0.018
2614.249	2614.237	0.012
2624.740	2624.731	0.009
2830.626	2830.614	0.012
2846.078	2846.070	0.008
2916.478	2916.474	0.005
3019.477	3019.474	0.003
3063.818	3063.811	0.006
3065.172	3065.166	0.006
3871.051	3870.933	0.118
3909.300	3909.210	0.089
3920.729	3920.647	0.083
3931.293	3931.222	0.071
4102.106	4101.946	0.159
4129.284	4129.150	0.134
4133.735	4133.624	0.111
4143.183	4143.068	0.115
4151.600	4151.498	0.103
4162.142	4162.044	0.099

– *Continued from previous page*

VMFCI (27535 cm^{-1})	Ref. (F13P7)	difference
4223.228	4223.215	0.013
4319.070	4319.057	0.013
4321.808	4321.790	0.019
4322.051	4322.034	0.018
4322.940	4322.921	0.019
4349.516	4349.407	0.109
4364.087	4363.994	0.093
4379.237	4379.154	0.084
4434.995	4434.982	0.014
4537.327	4537.314	0.012
4543.640	4543.624	0.016
4592.580	4592.507	0.073
4595.476	4595.411	0.065
4595.766	4595.701	0.065
5124.267	5123.631	0.636
5145.207	5144.629	0.578
5168.924	5168.468	0.456
5211.525	5211.157	0.368
5229.654	5229.343	0.310
5231.445	5231.127	0.319
5241.392	5241.107	0.285
5373.367	5372.724	0.643

– *Continued from previous page*

VMFCI (27535 cm^{-1})	Ref. (F13P7)	difference
5391.502	5390.914	0.587
5425.773	5425.302	0.470
5431.427	5431.026	0.401
5438.476	5438.080	0.396
5445.591	5445.219	0.371
5463.729	5463.400	0.329
5493.085	5492.987	0.097
5521.194	5521.132	0.063
5533.191	5533.137	0.054
5588.550	5588.459	0.091
5606.766	5606.500	0.266
5614.273	5613.989	0.285
5614.735	5614.448	0.287
5615.289	5615.235	0.053
5615.387	5615.311	0.076
5619.345	5619.111	0.233
5625.702	5625.652	0.051
5627.256	5627.195	0.061
5644.091	5643.699	0.393
5655.640	5655.326	0.314
5656.936	5656.589	0.347
5664.970	5664.677	0.294

– *Continued from previous page*

VMFCI (27535 cm^{-1})	Ref. (F13P7)	difference
5669.609	5669.295	0.313
5682.453	5682.183	0.270
5691.893	5691.625	0.267
5727.221	5727.153	0.068
5744.631	5744.586	0.046
5790.404	5790.365	0.039
5824.016	5823.959	0.057
5825.439	5825.400	0.039
5832.593	5832.514	0.079
5835.462	5835.394	0.068
5842.428	5842.388	0.039
5842.636	5842.593	0.042
5843.969	5843.919	0.050
5846.919	5846.873	0.046
5861.135	5861.059	0.077
5868.619	5868.402	0.217
5880.865	5880.607	0.258
5895.303	5895.069	0.234
5909.979	5909.755	0.224
5939.179	5939.163	0.016
5952.297	5952.271	0.026
5968.288	5968.277	0.010

– *Continued from previous page*

VMFCI (27535 cm^{-1})	Ref. (F13P7)	difference
6004.460	6004.417	0.043
6043.857	6043.824	0.033
6054.503	6054.480	0.023
6060.449	6060.421	0.028
6065.742	6065.703	0.038
6118.020	6117.835	0.185
6119.619	6119.439	0.180
6124.665	6124.502	0.164
	RMS	0.385

Approximate and reference energy levels (in cm^{-1}) of $2\nu_3$

J	irrep.	P0-P6 o2	Ref. (F13P7)	difference
1	F1	5978.86872	5978.86912	4.00e-04
1	E	6014.42282	6014.42253	-2.90e-04
1	F1	6014.43407	6014.43387	-2.00e-04
1	F2	6015.13600	6015.13658	5.80e-04
1	A2	6015.45383	6015.45497	1.14e-03
1	F2	6054.02780	6054.02775	-5.00e-05
1	F1	6054.16116	6054.16126	1.00e-04
2	F2	6000.08210	6000.08327	1.17e-03
2	E	6000.09006	6000.09121	1.15e-03
2	F2	6034.77683	6034.77645	-3.80e-04
2	F1	6034.79618	6034.79591	-2.70e-04
2	A1	6034.82061	6034.82050	-1.10e-04
2	F1	6035.88205	6035.88282	7.70e-04
2	E	6035.89135	6035.89222	8.70e-04
2	F2	6036.50223	6036.50425	2.02e-03
2	A2	6074.26929	6074.26891	-3.80e-04
2	F2	6074.45644	6074.45629	-1.50e-04
2	E	6074.64707	6074.64714	7.00e-05
2	F1	6074.84421	6074.84448	2.70e-04
2	A1	6075.03906	6075.03953	4.70e-04
3	A2	6065.45609	6065.45564	-4.50e-04

– *Continued from previous page*

J	irrep.	P0-P6 o2	Ref. (F13P7)	difference
3	F2	6065.47680	6065.47642	-3.80e-04
3	E	6065.49176	6065.49144	-3.20e-04
3	F1	6065.53439	6065.53425	-1.40e-04
3	A1	6066.97179	6066.97261	8.20e-04
3	F1	6066.99260	6066.99366	1.06e-03
3	F2	6067.00856	6067.00980	1.24e-03
3	E	6067.89629	6067.89931	3.02e-03
3	F1	6067.90049	6067.90353	3.04e-03
3	F2	6104.88789	6104.88727	-6.20e-04
3	F1	6105.23656	6105.23641	-1.50e-04
3	E	6105.51398	6105.51409	1.10e-04
3	F2	6105.78226	6105.78265	3.90e-04
3	F1	6106.15283	6106.15359	7.60e-04
4	F2	6106.48215	6106.48168	-4.70e-04
4	F1	6106.51248	6106.51207	-4.10e-04
4	E	6106.58121	6106.58093	-2.80e-04
4	F2	6106.59529	6106.59506	-2.30e-04
4	F1	6108.42637	6108.42743	1.06e-03
4	E	6108.45772	6108.45919	1.47e-03
4	F2	6108.46648	6108.46807	1.59e-03
4	A2	6108.47904	6108.48080	1.76e-03
4	F2	6109.62744	6109.63147	4.03e-03

– *Continued from previous page*

J	irrep.	P0-P6 o2	Ref. (F13P7)	difference
4	F1	6109.63865	6109.64270	4.05e-03
4	A1	6109.65244	6109.65653	4.09e-03
4	E	6145.74446	6145.74344	-1.02e-03
4	F1	6145.80070	6145.79975	-9.50e-04
4	A1	6146.21253	6146.21223	-3.00e-04
4	F1	6146.57171	6146.57172	1.00e-05
4	F2	6146.83582	6146.83609	2.70e-04
4	A2	6147.18397	6147.18454	5.70e-04
4	F2	6147.62785	6147.62888	1.03e-03
4	E	6147.68377	6147.68485	1.08e-03
5	F1	6128.30444	6128.30923	4.79e-03
5	E	6128.43992	6128.44450	4.58e-03
5	F2	6128.85892	6128.86274	3.82e-03
5	F1	6129.14876	6129.15218	3.42e-03
5	E	6157.81763	6157.81697	-6.60e-04
5	F1	6157.82839	6157.82773	-6.60e-04
5	A1	6157.86355	6157.86295	-6.00e-04
5	F1	6157.95804	6157.95743	-6.10e-04
5	F2	6157.98626	6157.98567	-5.90e-04
5	A2	6158.01034	6158.00977	-5.70e-04
5	F2	6160.20811	6160.20932	1.21e-03
5	E	6160.21324	6160.21454	1.30e-03

– *Continued from previous page*

J	irrep.	P0-P6 o2	Ref. (F13P7)	difference
5	F1	6160.25131	6160.25322	1.91e-03
5	F2	6160.26120	6160.26328	2.08e-03
5	A2	6161.67334	6161.67826	4.92e-03
5	F2	6161.68815	6161.69308	4.93e-03
5	E	6161.69865	6161.70358	4.93e-03
5	F1	6161.72993	6161.73489	4.96e-03
5	F2	6196.87977	6196.87808	-1.69e-03
5	F1	6196.98663	6196.98508	-1.55e-03
5	A1	6197.30356	6197.30227	-1.29e-03
5	F1	6197.96145	6197.96121	-2.40e-04
5	E	6198.23936	6198.23940	4.00e-05
5	F2	6198.52321	6198.52350	2.90e-04
5	A2	6199.21864	6199.21967	1.03e-03
5	F2	6199.51205	6199.51325	1.20e-03
5	F1	6199.61645	6199.61775	1.30e-03
6	A1	6192.98807	6192.99441	6.34e-03
6	F1	6193.31777	6193.32381	6.04e-03
6	F2	6193.67868	6193.68440	5.72e-03
6	A2	6194.29779	6194.30264	4.85e-03
6	F2	6194.87121	6194.87563	4.42e-03
6	E	6194.97122	6194.97550	4.28e-03
6	F2	6219.45496	6219.45378	-1.18e-03

– *Continued from previous page*

J	irrep.	P0-P6 o2	Ref. (F13P7)	difference
6	F1	6219.47706	6219.47589	-1.17e-03
6	A1	6219.60195	6219.60055	-1.40e-03
6	F1	6219.66472	6219.66339	-1.33e-03
6	E	6219.69491	6219.69358	-1.33e-03
6	F2	6219.73567	6219.73430	-1.37e-03
6	A2	6222.29551	6222.29666	1.15e-03
6	F2	6222.30142	6222.30273	1.31e-03
6	F1	6222.30717	6222.30863	1.46e-03
6	A1	6222.34505	6222.34725	2.20e-03
6	F1	6222.34882	6222.35115	2.33e-03
6	E	6222.35039	6222.35277	2.38e-03
6	F2	6224.04062	6224.04620	5.58e-03
6	F1	6224.06324	6224.06879	5.55e-03
6	E	6224.12300	6224.12851	5.51e-03
6	F2	6224.13369	6224.13920	5.51e-03
6	A2	6258.26341	6258.26049	-2.92e-03
6	F2	6258.34048	6258.33768	-2.80e-03
6	E	6258.39352	6258.39082	-2.70e-03
6	F1	6258.91890	6258.91669	-2.21e-03
6	F2	6259.84444	6259.84382	-6.20e-04
6	E	6260.13940	6260.13903	-3.70e-04
6	F1	6260.41911	6260.41903	-8.00e-05

– *Continued from previous page*

J	irrep.	P0-P6 o2	Ref. (F13P7)	difference
6	F2	6261.38435	6261.38535	1.00e-03
6	E	6261.86122	6261.86242	1.20e-03
6	F1	6261.91178	6261.91304	1.26e-03
6	A1	6261.98465	6261.98597	1.32e-03
7	F1	6269.42277	6269.43037	7.60e-03
7	E	6269.95729	6269.96471	7.42e-03
7	F2	6270.37772	6270.38514	7.42e-03
7	A2	6271.79778	6271.80479	7.01e-03
7	F2	6272.21209	6272.21816	6.07e-03
7	F1	6272.41698	6272.42263	5.65e-03
7	A2	6291.36944	6291.36725	-2.19e-03
7	F2	6291.38885	6291.38667	-2.18e-03
7	E	6291.40080	6291.39865	-2.15e-03
7	F1	6291.59991	6291.59720	-2.71e-03
7	F2	6291.70511	6291.70253	-2.58e-03
7	E	6291.76985	6291.76710	-2.75e-03
7	F1	6291.79295	6291.79019	-2.76e-03
7	F2	6294.67864	6294.67972	1.08e-03
7	E	6294.68453	6294.68584	1.31e-03
7	F1	6294.68544	6294.68688	1.44e-03
7	A1	6294.68670	6294.68833	1.63e-03
7	F2	6294.72068	6294.72317	2.49e-03

– *Continued from previous page*

J	irrep.	P0-P6 o2	Ref. (F13P7)	difference
7	F1	6294.72121	6294.72363	2.42e-03
7	E	6296.69332	6296.69913	5.81e-03
7	F1	6296.70175	6296.70753	5.78e-03
7	A1	6296.72655	6296.73226	5.71e-03
7	F1	6296.82124	6296.82683	5.59e-03
7	F2	6296.84500	6296.85054	5.54e-03
7	A2	6296.86613	6296.87164	5.51e-03
7	F2	6330.01416	6330.00945	-4.71e-03
7	F1	6330.08421	6330.07961	-4.60e-03
7	E	6330.79575	6330.79197	-3.78e-03
7	F2	6330.89423	6330.89058	-3.65e-03
7	A2	6331.94810	6331.94650	-1.60e-03
7	F2	6332.24950	6332.24818	-1.32e-03
7	F1	6332.51103	6332.50998	-1.05e-03
7	A1	6332.79522	6332.79444	-7.80e-04
7	F1	6333.88574	6333.88629	5.50e-04
7	E	6333.97400	6333.97464	6.40e-04
7	F2	6334.59698	6334.59783	8.50e-04
7	F1	6334.66138	6334.66231	9.30e-04
		RMS		0.003